P 3 mil

NASA TECHNICAL TRANSLATION

NASA TT F-816

NASA TT F-816

(NASA-TT-F-816) THE METEOROLOGY OF MARS (Scripta Technica, Inc.) 72 p HC $3.75 CSCL 03B
N74-20526
Unclas
H1/30 30578

APR 1974

THE METEOROLOGY OF MARS

by K. Ya. Kondrat'yev and A. M. Bunakova

Hydrometeorological Press
Leningrad, 1973

NATIONAL AERONAUTICS AND SPACE ADMINISTRATION • WASHINGTON, D. C. • APRIL 1974

1. Report No. NASA TT F-816	2. Government Accession No.	3. Recipient's Catalog No.
4. Title and Subtitle THE METEOROLOGY OF MARS		5. Report Date April 1974 6. Performing Organization Code
7. Author(s) K. Ya. Kondrat'yev and A. M. Bunakova		8. Performing Organization Report No. 10. Work Unit No.
9. Performing Organization Name and Address Scripta Technica, Inc. Washington, D. C. 20005		11. Contract or Grant No. NASw-2484 13. Type of Report and Period Covered Translation
12. Sponsoring Agency Name and Address National Aeronautics and Space Administration Washington, D. C. 20546		14. Sponsoring Agency Code

15. Supplementary Notes

Translation of "Meteorologiya Marsa," Leningrad, Hydrometeorological Press, 1973, 62 pp.

16. Abstract

The principal features of the Martian weather are described for analysis of the problem of this planet's meteorology, for comparison of planets of the terrestrial group in regard to the specifics of their weather. Unsolved problems of Martian meteorology and the prospects for further research are briefly discussed.

STAR Category 30

17. Key Words (Selected by Author(s))	18. Distribution Statement Unclassified-Unlimited CAT.-30		
19. Security Classif. (of this report) Unclassified	20. Security Classif. (of this page) Unclassified	21. No. of Pages 70	22. Price* $3.75

*For sale by the National Technical Information Service, Springfield, Virginia 22151

ANNOTATION

With the success of direct measurements made with instruments lowered into the atmosphere of Mars and landed on its surface and remote indication of the properties of the atmosphere and surface from spaceprobes in orbit around the planet, our conceptions as to the properties of the atmosphere and surface of this planet havebeen radically enriched. The available experimental data, which are based on results obtained with the Mars 2 and 3 and Mariner 6, 7, and 9 spaceprobes, enable us to form a rather complete picture of the meteorological regime of Mars. Numerical modeling of the general circulation of the Martian atmosphere has made an important contribution to the development of research on the weather on Mars. Taken together, all of these things form a basis for analysis of the principal features of the Martian weather, as characterized by the space-time variability of atmospheric pressure, temperature, wind, clouds and certain other parameters. The principal features of the Martian weather are described not only for analysis of the problem of this planet's meteorology, but also for comparison of planets of the terrestrial group in regard to the specifics of their weather. Unsolved problems of Martian meteorology and the prospects for further research are briefly discussed.

/2*

*Numbers in the margin indicate pagination in the foreign text.

PRECEDING PAGE BLANK NOT FILMED

TABLE OF CONTENTS

PRECEDING PAGE BLANK NOT FILMED

INTRODUCTION

/3

Recent years have been marked by strong interest in investigation of Venus and Mars, the planets nearest the earth. The rapid development of earth-based methods for study of the atmospheres and surfaces of these planets (primarily infrared spectroscopy and radio astronomy) have made it possible to acquire a whole series of important results. However, there is no doubt that the experiments on the spaceprobes of the "Venera," "Mars," and "Mariner" series have made a decisive contribution to the study of Venus and Mars. As things developed, the most radical changes in our concepts as to the nature of the nearest planets resulted from direct measurements of structural parameters and compositions by instruments lowered through the atmospheres of the planets and landed on their surfaces [1-4]. Scientific programs carried out with the aid of spacecraft orbiting the planets have also been an important factor. This approach has the advantage of planetary-scale coverage of the phenomena of interest.

As was observed in [54], the placing of Soviet and American spaceprobes equipped with mutually complementary scientific instrument packages in orbit around Mars, their simultaneous functioning for extended periods, and exchange of information between Soviet and American scientists while the experiments were still in progress have significantly advanced the investigation of Mars.

The accumulation of data on the conditions prevailing in the atmospheres and on the surfaces of the planets makes possible an approach to planned study of features of their weather and climate. Although only a few years ago this formulation of the problem was possible only within the framework of a popular-science exposition [5], we now have extensive material that permits analysis of this problem on a quite serious basis. We are also aided here by progress in theoretical research devoted to numerical modeling of the general circulation of the atmospheres of the planets nearest the earth.

It must be stressed that interest in study of the laws of weather and climate on other planets is determined to a substantial degree by the importance of this kind of research from the standpoint of the "comparative meteorology" of planets of the terrestrial group [9, 51-53, 56, 57, 59]. In many respects (mass, radius, density, etc.), Venus, the earth, and Mars exhibit distinct similarities. During recent years, however, a whole series of significant differences among these planets has also come to light. Thus, our conceptions of Venus have undergone a far-reaching and, in certain cases, unexpected evolution as a

result of direct measurements made with the "Venera" spaceprobes /4
and the "Mariner" radio-occultation data. In addition to the high (over 600°K) temperature of Venus, which distinguishes it sharply from the earth, spectroscopic data indicate a very low water-vapor content above the cloud cover, and radio-astronomical measurements point to a low water-vapor content in the lower layers of the Venusian atmosphere (the total water-vapor content in the Venusian atmosphere appears to be smaller by a factor of 10^3 to 10^4 than that in the earth's biospherere). Another distinctive property of Venus is its very slow (and "backward") axial rotation. The specifics of cloud conditions on the planets are highly characteristic. Of special importance for the weather on Mars are its dust storms, which sometimes envelop the entire surface of the planet (as was the case, for example, at the end of 1971).

Common features of the terrestrial and Martian atmospheres are the significant influence of the Coriolis force and the presence of annual variations of the meteorological elements. Important differences consist in the absence of oceans on Mars, the small amount of water vapor on that planet, and its lack of a stable cloud cover. The low density of the Martian atmosphere near the surface and the predominance of carbon dioxide result in a radiative relaxation constant approximately 1/10 as large as that of the earth; this indicates a much greater importance of radiative processes as factors determining the general circulation of the atmosphere (in contrast to the cases of Venus and Jupiter).

The above differences and similarities of the planets are of great interest from the standpoint of comparative meteorology, our understanding of the laws of evolution of the planets, and more profound study of the processes in the earth's atmosphere, which are governed by the complex interaction of various factors (dynamic, radiative, the influence of the planet's rotation, etc), while, for example, radiation effects are dominant for the atmospheric circulation on Mars and dynamic factors are decisive for Venus and Jupiter. A significant difference in the latter case consists in the fact that Venus rotates very slowly and Jupiter rapidly [6].

The occurrence of dust storms and the "radiation-governed" general circulation of the Martian atmosphere make it possible to investigate the effects of atmospheric aerosol contaminants on the meteorological regime, which characterizes the peculiarities of the weather on this planet. The investigation of such a model may be of great interest from the standpoint of analysis of the possible effects of human activity on the earth's climate [7, 8]. The "antigreenhouse effect" of the Martian dust noted in [54] arises out of the fact that the surface is cooled

during a dust storm and the temperature of the atmosphere is raised as a result of absorption of solar radiation by the dust. A similar phenomenon is also observed under the conditions of the earth's atmosphere [55].

Investigation of the Venusian atmosphere is of special interest for understanding of the earth's less thoroughly investigated tropical circulation (in which the Coriolis forces are small). Thus far, no adequate explanation has been found /5 for the structural features and composition of the Venusian atmosphere. For example, it cannot be considered a proven fact that the high surface temperature of Venus is due to the greenhouse effect. A sound basis for this hypothesis will become possible only after study of data on the vertical temperature profiles and solar radiation flux deep in the atmosphere, on the temperature field of the planet's surface, etc. Our information on the nature of the surface and core of Venus is highly fragmentary. Radar measurements indicate that the surface is quite flat (its height varies through ± 1.5 km, and a peak 2.5 km high has been registered only in one case) and has the dielectric constant typical of silicates. There are no indications that anything similar to the earth's continents and oceans exists on Venus. Its atmosphere is composed almost entirely of CO_2 with very small admixtures of H_2O, CO, HCl and HF (it is interesting to note that attempts to detect such gases as H_2S, COS, SO_2, and SO_3 have not succeeded), and inferences as to the nature of the two-layered cloud cover have been most contradictory. The inadequacy of our information on the composition of the atmosphere's lower layers (detailed mass-spectrometer measurements are called for) and of the temperature and humidity profiles and our lack of data on the wind preclude the establishment of laws governing the shaping of the structure and composition of the Venusian atmosphere. All of this makes it difficult to analyze weather conditions on Venus.

Our information on Mars is much more complete, especially since the successful completion of the "Mars 2," "Mars 3" [4, 11], and "Mariner 9" missions [12]. Although much remains unclear concerning the meteorology of Mars, the basic characteristics of the weather, expressed in the form of distributions of temperature, atmospheric pressure, clouds, and certain other meteorological parameters, have been quite clearly resolved. It is this fact that determined the choice of subject matter for the present booklet, whose purpose is to analyze weather conditions on Mars on the basis of recent experimental data and numerical-modeling results.

The weather and climate of a planet are determined by the amount of incoming solar radiation, the physical properties (and topography) of the underlying surface, and the composition and physical properties of its atmosphere. The solar constant is quite accurately known for Mars: it is 0.85 cal$\cdot$ $\cdot cm^{-2} \cdot min^{-1}$.

Chapter I discusses our information on the composition and physical characteristics of the Martian atmosphere according to "Mars 2," "Mars 3," and "Mariner 9" spaceprobe data and presents a brief description of the Martian topography. Patterns in the general circulation of the atmosphere that have been obtained by numerical modeling form the subject of Chapter II. Chapter III presents a conception of the outgoing radiation field and radiation budget of the planet and certain structural and composition features of the atmosphere that have been obtained by analysis of data on the radiation field. The prospects for future research are discussed in the conclusion.

CHAPTER I

/6

RESULTS OF SCIENTIFIC EXPERIMENTS ON THE "MARS 2," "MARS 3," AND "MARINER 9" SPACEPROBES

The coordinated research program carried out by the spaceprobes employed a strategy of saturation, and included television observations, IR spectroscopy, IR radiometry, UV spectroscopy, radiooccultation measurements, and experiments in celestial mechanics.

The result was acquisition of a large volume of scientific data on the physical properties of the planet's surface and atmosphere and of the space near the planet. Much more time will be required for complete reduction of all of the data obtained and their comprehensive analysis. Only the first results are stated in existing publications.

In this chapter, we shall present a brief summary of the basic results obtained from the spaceprobes "Mars 2," "Mars 3" [11, 54] (which were launched on 19 and 28 May 1971, respectively), and "Mariner 9" [12, 73, 75] (launch date 30 May 1971).

Most important, of course, is the information on the planet itself. These include results from study of the Martian topography, surface- and soil-temperature measurements, and the composition and structure of the atmosphere.

As we know, the experiments were performed in a totally unexpected meteorological situation: a powerful dust storm was observed while the spaceprobes were functioning on Mars. According to earth-based observations, it began in September and reached its peak toward the end of October. Substantial abatement of the storm did not begin until the second half of December, and the storm had subsided practically completely about a month later. Severe dust storms have been observed in the past at several great oppositions, but none has approached the force of this one.

All instruments on the spaceprobes registered changes in the characteristics of the planet's atmosphere that were associated with the storm. Only in the region of the south polar cap and in certain mountainous areas of the planet were the amounts of dust substantially smaller.

§1. THE MARTIAN TOPOGRAPHY

/7

Various measurement techniques have been used to investigate the Martian topography [4, 13-18, 54, 58, 73]: earth-based radar measurements and radiooccultation, infrared, and ultraviolet measurements from the "Mars 2," "Mars 3," "Mariner 6,"

"Mariner 7," and "Mariner 9" spaceprobes. Television pictures of the surface provide a very clear qualitative presentation of the Martian relief [2, 12, 72]. Our most extensive sufficiently reliable quantitative data have been obtained by reduction of measurements of the ultraviolet radiation reflected by Mars, which enables us to determine first the pressure field at surface level and then (by assigning a lapse rate in the atmosphere) the topography of the terrain. The possibility of determining the pressure results from the fact that the surface albedo of the Martian deserts is very low, so that the radiation reflected into space (and especially its variations) are determined by molecular scattering in the atmospheric layer (in the absence of dust in the atmosphere). In turn, the intensity of molecular scattering depends on the density of the medium.

About 400 spectra were registered for the sunlit side of the planet with ultraviolet spectrometers on the "Mariner 6" and "Mariner 7" spaceprobes [13]. Spectra in the 1900-4300 Å band were registered at 3-second intervals (the spectral resolution was about 20 Å). The field of the spectrometer (0.23° × × 2.3°) provided spatial resolutions ranging from 30 × 300 km near the bright limb of the planet to 14 × 140 km for the shortest distance to the planet (the long axis of the field was oriented perpendicular to the line to the sun).

The observations indicated that there are only small variations of the spectral radiation distribution in the desert regions for $\lambda < 3500$ Å (reflectivity is always observed to increase with decreasing wavelength), so that the photometric properties depend weakly on wavelength in this case. For this reason, analysis of the data was confined to a 100 Å interval centered on 3050 Å, which can be regarded as representative for the 2600-3500 Å region. Measurements of the brightness coefficient R (reflectivity) pertaining to phase angles from 46 to 91° and selected for four areas of the Martian surface on which the surface albedo can be regarded as constant made it possible to determine the parameters of the Minnaert function:

$$R = R_0 \mu_0^k \mu^{k-1}, \qquad (1)$$

where $R = \pi B/F$ (B is the measured brightness and F is the solar radiation flux), μ_0 and μ are the cosines of the incidence and reflection angles of the solar radiation, and R_0 and k are parameters determined from the observations.

The reflectivity of Mars is determined by two components: /8
reflection from the surface, which can be determined from (1), and atmospheric scattering, which can be represented in the form $\frac{p}{4}\frac{\tau}{\mu}$ ($p(\psi)$ is the normalized scattering function, which depends on the scattering angle ψ, and τ is the optical thick-

ness of the atmosphere).

The atmospheric pressure can be written

$$p=\frac{p_0}{\tau_0}\tau. \qquad (2)$$

Here (assuming a pure atmosphere consisting of carbon dioxide) $\tau_0 = 0.032$ at $p_0 = 6.0$ mb.

Taking attenuation and multiple scattering into account, we present the expression for the reflectivity at 3050 Å in the form

$$R=f\left\{\left(\frac{p}{4}\right)\left(\frac{\tau}{\mu}\right)\left[\frac{1-\exp(-\tau M)}{\tau M}+R_0\mu_0^k\mu^{k-1}\exp(-\tau M)\right]\right\},$$

where $M=\frac{1}{\mu_0}+\frac{1}{\mu}$ and f is a coefficient that characterizes the influence of multiple scattering and depends on μ, μ_0, τ and ψ (the dependence on τ is strongest on Mars when R_0 and τ are small). The coefficient f can be determined by comparison with the exact solution in simplified cases. In the case under consideration, it was assumed that f = 1.

With (2) and (3), we obtain

$$p=\frac{p_0}{\tau_0}\frac{1}{M}\ln\left[\frac{R_0\mu_0^k\mu^{k-1}-R_A}{R-R_A}\right],$$

where $R_A = p/4\mu M$. This formula can be used to determine p from known values of τ_0/p_0, R_0, k, and $p(\psi)$.

The results of independent determination of the pressure from measurements in the infrared were used to check the reliability of the method described above and to adapt the parameters [15]. Pressure data yield information for study of the topography of the Martian surface, and these data were compared with the results of the infrared measurements. The average pressure according to ultraviolet measurements (337 points) was 5.8 mb, while the infrared measurements indicated 5.3 mb. The discrepancy can be explained by the imperfect congruence of the fields of the instruments.

Reduction of "Mariner 9" measurements of the ultraviolet radiation reflected by Mars in a 100 Å spectral interval centered around 3050 Å during the period from 14 November 1971 through 1 March 1972 yielded more extensive information on the atmospheric-pressure distribution over the surface of the planet (the field of the modified spectrometer on "Mariner 9" covers a 10 × 30-km area on the surface in sightings from a distance of 3400 km) [18].

During the dust storm, which continued to the beginning of January 1972, scattering of solar radiation by the optically dense layer of dust made the dominant contribution to the reflected radiation. By 23 January, however, the atmosphere had become quite transparent and optically thin at 3050 Å, and this made it possible to use reflected-radiation data to determine the pressure from this time on. /9

Under dust-storm conditions, the reflectivity is accurately described by

$$R=\frac{p(\psi)\,\tilde{\omega}_0}{4}\,\frac{\mu_0}{\mu+\mu_0},$$

where $\tilde{\omega}_0$ is the albedo for single scattering. The parameter $p\tilde{\omega}_0$ equals 0.2 for the entire period from 13 November 1971 to 1 January 1972.

Deviations of the calculated from the measured values occur only near the limb (small μ) and terminator (small μ_0), when the plane-parallel-atmosphere approximation is not valid. During the dust storm, the atmosphere was most transparent in the region of the south polar cap, where its optical thickness was about one.

When the storm was over, observing conditions were similar to those that had prevailed during the life of the "Mariner 6" and "Mariner 7" spaceprobes in 1969. The dominant contribution of Rayleigh scattering to the reflectivity variations enables us in this case to determine atmospheric pressure from reflected-radiation intensity using absolute pressure values obtained from radiooccultation measurements to establish correspondence between reflectivity and pressure. The four parameters in relation (4) were found by least squares for 56 points, at which the pressure was determined by the radiooccultation method. The rms disagreement between the "ultraviolet" and "radiooccultation" pressures was 16% in the pressure range from 2.6 to 8.1 mb.

It was possible in [8] to construct a chart of the areographic pressure distribution in the latitude belt from 50°S to 20°N. The most distinct pressure maximum (about 10 mb) is observed in the Tharsis region (at approximately 100°W, 0°N). A distinct minimum occurs in the Hellas region (290°W, 45°S).

The pressure data were used to obtain the topography of the surface on the assumption that the scale height equals 10 km. The 6.1-mb level was taken as zero elevation. A topographic map of Mars appears in Fig. 1. Comparison with television pictures confirmed that the "ultraviolet" topogra-

phy is realistic. Detailed profiles of the relief in the Tharsis region indicate the existence here of sharp elevation changes in the range from −0.5 to 9 km. The elevations vary from less than −2 km to more than 10 km (the highest elevations range up to 14 km according to the infrared measurements [73]). Thus, the topography of Mars is quite similar to that of the earth in regard to the amplitude of its height variations. /10 At the same time, the absence of seas and oceans and the presence of many craters resembling those on the moon make the Martian topography highly specific.

The results described above agree closely with "Mars 2" and "Mars 3" spaceprobe measurements [54]. Reduction of the measurement results by means of an infrared photometer working in the 2.06-μm carbon dioxide absorption band indicated that the pressure on Mars at mean surface level is 5.5-6.0 mb. The pressure variations in the equatorial region indicate the existence of a 12-14-kilometer range of elevations extending over large areas. The data for 16 February 1972 indicate that along the spaceprobe's path over, for example, the Hellespontus region, the elevation above mean surface level is 2-3 km, and that it drops to 1 km below mean surface level toward the Hellas region. Then there is a marked rise in the direction of the dark areas of Iapygia and Syrtis Major, up to 3 km. The elevations decrease to the north of Syrtis Major.

Study of features of the behavior of the Martian surface temperature field in space and time on the basis of infrared-radiometer measurements (sensitivity range 8-40 μm) led to the conclusion that the thermal conductivity of the Martian soil is low, corresponding to dry sand or dry dust in a rarefied atmosphere (the Martian surface chills very rapidly after sunset). Measurements of radio emission at 3.5 cm, which indicate that there is no diurnal temperature variation at depths on the order of 30-50 cm, also indicate high thermal inertia and low thermal conductivity of the soil.

§2. THE LOWER ATMOSPHERE /11

Chemical Composition. According to IR and UV spectroscopy, the basic component of the Martian (as of the Venusian) atmosphere is carbon dioxide — a respect in which it differs substantially from the earth's (Table 1). Traces of H_2O have been detected along with the CO_2: water-vapor rotational bands have been identified in "Mariner 9" outgoing thermal radiation spectra (see Fig. 3). The "Mars 3" photometer, which was designed for measurements in the water-vapor absorption band around 1.38 μm, showed [74] that the water-vapor content did not exceed 5 μm of precipitable water throughout the entire time of the experiment (compared to

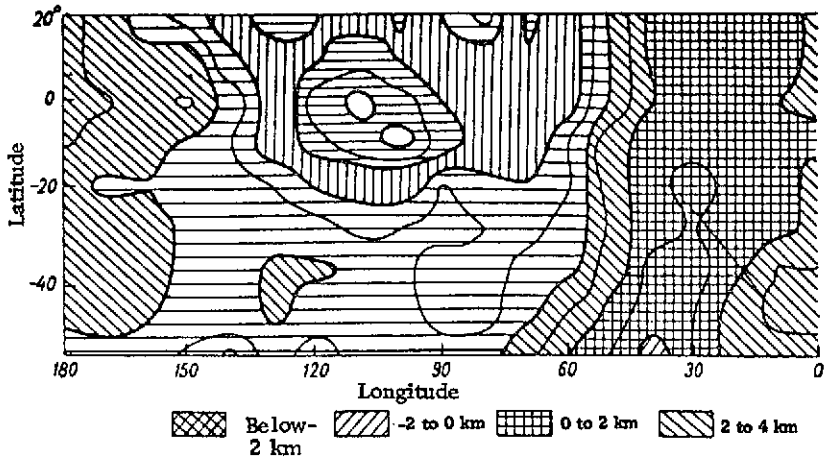

Figure 1. Topographic

several times as much in the earth's atmosphere). According to "Mariner 9" data, the average water-vapor content varied in the range 10-20 μm [73]. It had been assumed on the basis of earth-based indirect measurements made in advance of the space-probe flights that the Martian atmosphere contained up to 50 μm of precipitable water. It may be that the extreme dryness of the Martian surface that was observed by the spaceprobes is due to anomalously strong "capture" of water vapor by the North Polar Cap, which reached more southerly latitudes than in past observations. Nor can we exclude the effects of the anomalously severe dust storm, which could have been manifested in adsorption of water vapor on the dust particles and subsequent removal of the water vapor from the atmosphere as the particles settled onto the surface. No large-scale space-time variations of water-vapor content were observed anywhere in the southern hemisphere during the period from November 1971 through April 1972. However, water vapor was not registered at high latitudes in the northern hemisphere either. /12

In a number of the investigations, attempts were made at experimental determination of the contents of minor components in the Martian atmosphere, or at least at estimation of the possible upper limits of their contents. Thus, for example, the basic objective of a "Mariner 6" and "Mariner 7" IR spectroscopy experiment [69] was to investigate the composition of the Martian atmosphere, including possible minor components, in spectra of the planet in the band from 1.88 to 14.4 μm. The spectrometer was calibrated in advance in the laboratory by recording absorption spectra and obtaining growth curves for various gas mixtures in a cell with total ray paths up to 2543 meters, which modeled the possible conditions of the Martian atmosphere (all minor components were

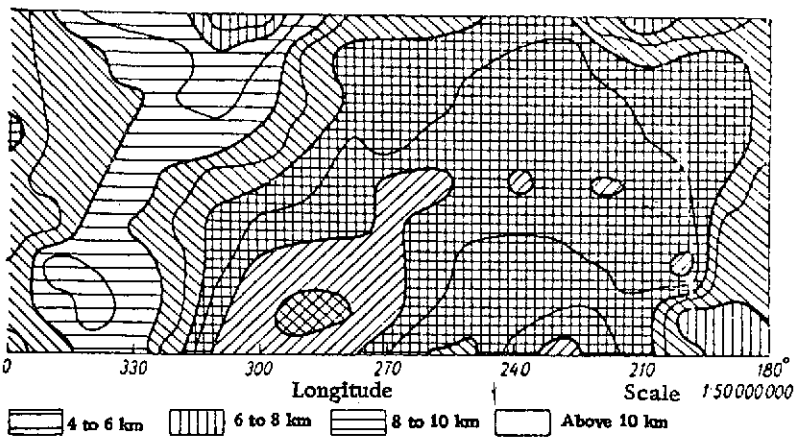

Map of Mars.

studied in mixtures with carbon dioxide at a pressure of 5.6 mb and room temperature).

The actual Martian spectra were interpreted with the purpose of determining the possible upper content limits of the minor constituents. The registered spectra contained clear indications of the presence of only three components: carbon dioxide (the principal component), carbon monoxide, and water vapor. The possible upper content limit of other minor constituents were found from the laboratory-calibration data, and had the following values (the first figure characterizes the total content of the gas in cm-atm at standard pressure and temperature, and the second the volume concentration in parts per million): NO_2 (< 0.0016; 0.23), NH_3 (< 0.003; 0.44), C_3O_2 (< 0.0032); 0.45), SO_2 ($\leq$ 0.0037; 0.52), COS (< 0.0040); 0.56), NO (< 0.0050; 0.70), O_3 (< 0.0061; 0.86), CH_4 (< 0.026; 3.7), N_2O (< 0.13; 18), HCl (< 3.7; 520), HBr (< 8.2; 1150), H_2S (< 27; 3800).

The figures were supplemented by an analysis of available spectroscopic data to obtain estimates of the upper content limits of 27 minor constituents for which no laboratory measurements of the growth curves had been made. According to the results of this analysis, the concentrations of the following components do not exceed 1.0 ppm (which corresponds to contents less than 0.0071 cm-atm): SF_6, NF_3, Cl_2CO, CF_4, CHF_3, Br_2CO and SiF_4. The concentrations of C_2F_6, CO_3, F_2CO, C_2H_4, BF_3, CS_2, $CHCl_3$, C_2H_6, H_2CO, CH_3F, C_6H_6, and CH_2I_2 are less than 6.0 ppm (contents below 0.035 cm-atm), and those of

TABLE 1. CERTAIN DATA ON PLANETS OF THE TERRESTRIAL GROUP

Planet	Albedo A	Distance from Sun a.u.	Radius R, km	Equilibrium Temperature T_e, °K	Dominant Gas	Molecular Weight	Acceleration of Gravity g/(sec·cm^2)	Pressure P_0 at Surface, bar
Venus	0.85	0.723	6050	205	CO_2	44.0	884	100
Earth	0.40	1.000	6371	246	N_2; O_2	29.2	982	1.013
Mars	0.15	1.523	3394	259	CO_2	44.0	376	0.006

C_2H_2, HCN, CH_2Br_2, CH_2Cl_2, CH_3Br, PH_3, CH_3Cl and CH_3I are less than 50 ppm (< 0.35 cm-atm). These values are comparable with those obtained earlier from earth-based measurements.

TABLE 2. RANGES OF VARIATION OF PRESSURE AND TEMPERATURE AT SURFACE OF MARS, ACCORDING TO MARINER 4, 6, 7, AND 9 SPACEPROBE DATA

Parameter	Mariner 4		Mariner 6		Mariner 7		Mariner 9	
	from	to	from	to	from	to	from	to
Pressure, mb	4.5	8.0	3.0	7.6	3.5	7.5	2.9	8.3
Temperature, °K	160	210	153	297	185	290	195	225

Data for C_3O_2 and CO_3 are of special interest from the standpoint of investigating photochemical processes in the Martian atmosphere. It has been suggested concerning the first of these substances that its polymer might be the basic constituent of the Martian surface. The low maximum C_3O_2 content indicates that there is little justification for this hypothesis. Neutral CO_3 molecules have been regarded as a possible product of a reaction in the atmosphere between oxygen atoms and carbon dioxide molecules with importance as an intermediate in the recombination of oxygen atoms and carbon monoxide molecules. The establishment of an upper content limit for CO_3 amounting to less that 0.0088 cm-atm should be significant for investigation of the validity of this hypothesis. /13

It was reported in [70] that data on the highest possible hydrogen sulfide and sulfur dioxide contents indicate that modern volcanic activity on Mars is unlikely.

A result of the presence of dust is the appearance of SiO_2 bands in the infrared emission spectrum as structural features of the spectrum in the 400-600 cm^{-1} and 850-1250 cm^{-1} bands [73]. The Martian spectrum agrees with the laboratory spectrum of terrestrial minerals in regard to the SiO_2

content, which lies in the range 60 ± 10% (compared with the earth's volcanic rocks).

Surface temperature. The surface temperature of Mars, measured at various latitudes and various times, is one of the important climatic characteristics. Inferences may be drawn as to the properties of the material composing the soil from the diurnal and spatial variations of surface temperature. Table 2 gives the limits of surface-temperature and atmosphere-pressure variability obtained from "Mariner" spaceprobe data.

For measurement of surface temperature, the "Mariner 9" spaceprobe carried a two-channel (wavelengths 10 and 20 μm) IR radiometer of the same type that had been used previously on "Mariner 6" and "Mariner 7" [12]. The field of the radiometer coincides with that of a high-resolution television camera, occupying about two thirds of the latter's area. The spatial resolution of the radiometer at periapsis is about 20 km, and its temperature resolution approximately 0.5°K. Preliminary analysis of the results showed that the brightness temperatures measured from "Mariner 9" differ substantially from those obtained on the "Mariner 6" and "Mariner 7." While the 1969 data were easily explained by emission from the Martian surface (the effect of the atmosphere was of little consequence), the results obtained in 1971 point to a considerable influence of the atmospheric dust. This is reflected especially clearly in the features of the diurnal temperature variation, whose amplitude was found to be much smaller than in the absence of an atmospheric effect, and to diminish in the direction toward the South Pole. /14

Television pictures indicate that the zone of the South Pole and certain other regions were relatively free of dust. The residues of the Polar Cap form the most easily observed phenomenon. They are about 35°K colder than the surrounding regions. The "Mariner 7" data indicated a surface temperature of about 148°K for the region of the South Polar cap in early spring (which corresponds to the sublimation temperature of carbon dioxide). This permitted the conclusion that the polar caps consist of solid carbon dioxide. "Mariner 9" results pertaining to the receding polar cap (second half of summer) indicated temperature values approximately 25°K higher (according to the television pictures, these values pertain to a surface 90% covered by deposits having a high albedo). Since the increase in radiation temperature cannot be ascribed to dust (because of the small dust content), the possibility that these deposits are frozen water cannot be excluded.

We should note in this context that analysis of "Mariner 9"

television pictures indicated the existence of branching and meandering canyons that could attest to the existence of liquid water on Mars in the recent geological past [66, 71].

Having analyzed "Mariner 7" measurements of the ultraviolet radiation reflected from the region of the South Polar cap, K. Pang and C. Hord [62] arrived at the following conclusions: 1) the atmosphere of Mars consists of carbon dioxide; 2) if the surface temperature drops below 148°K, carbon dioxide sublimates onto the surface and layers of ice are formed; 3) at the same time, carbon dioxide condensing in the atmosphere forms clouds; 4) the fall of "snow" from the clouds contributes to the formation and thickening of the polar cap; 5) sublimation on the surface continues even after the "snowfall" has stopped, with the result that the surface becomes specular; 6) the clouds dissipate in early spring, exposing the polar cap to direct solar irradiation. /15

In the Tharsis region (11°N, 119°W), "Mariner 9" television pictures showed a dark zone for which radiometeric measurements yielded a diameter of about 300 km and a temperature 8°K higher than that in the surrounding regions. If we assume this to be due to the absence of the dust haze in this area and intensified warming of the surface due to the high atmospheric transparency, and remember that radar measurements indicated the existence of a crest 8 km high in the Tharsis region, this will enable us to estimate the height of the dust layer.

According to data from the "Mars 2" and "Mars 3" IR radiometers, which measured the radiation of the planet in the wavelength range λ = 8-40 μm, temperature varied in a broad range as a function of the aerographic coordinates and time: from 286°K (for 1400 hours local solar time at 11°S) to 180°K (for 1900 hours local solar time, 19°N). The temperature dropped to 163°K in the region of the North Polar cap.

The fact that the diurnal temperature variation was found to be smaller that was expected can be explained qualitatively only by considering the influence of the dust, which has absorption and radiation coefficients $\beta_{abs} = \beta_{rad} = 0.5$, and assuming that the thickness of the dust layer decreases toward the South Pole.

The low nocturnal temperatures indicated by "Mars 2" and "Mars 3" indicate that the surface of Mars cools very rapidly after sunset and, consequently, that the thermal conductivity of the soil is very low [54]. Quantitative estimates indicate that this is consistent with dry sand or dry dust in a rarefied atmosphere.

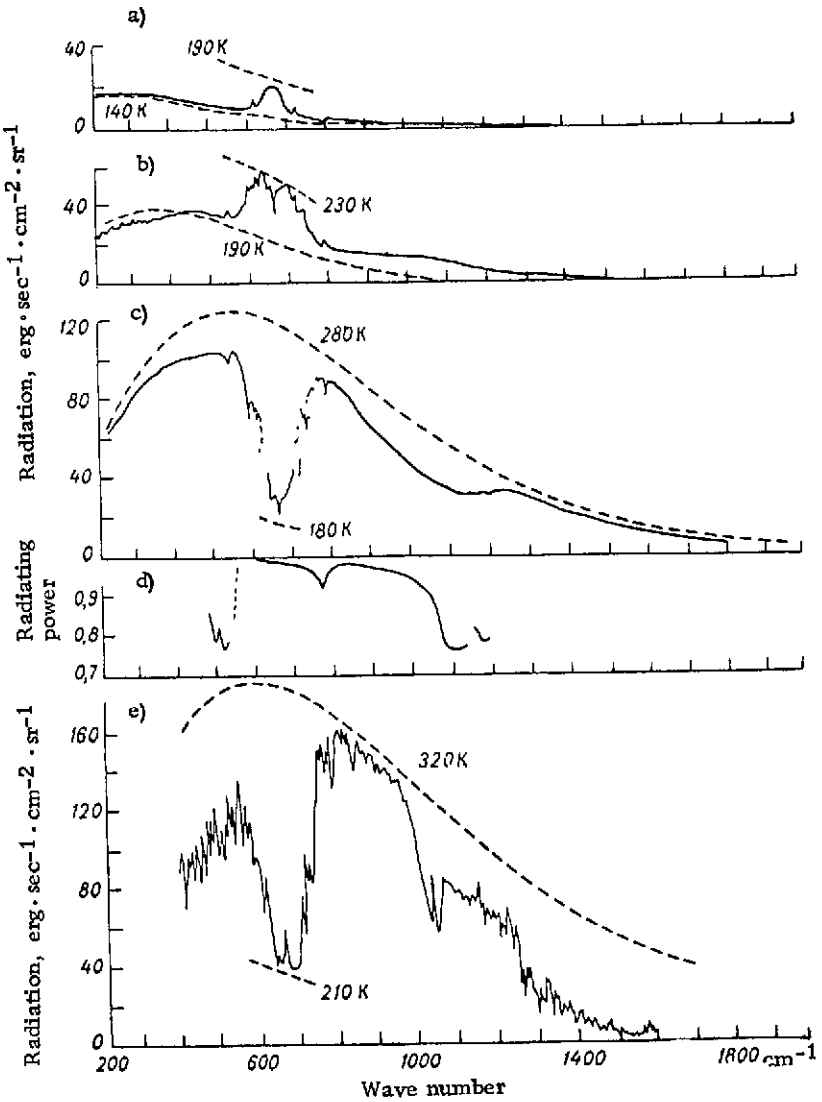

Figure 2. Thermal Radiation Spectra. a) Spectrum of radiation from North Polar cap of Mars, 102nd orbit; b) spectrum of radiation from South Polar cap of Mars, 30th orbit; c) radiation spectrum of Mars for middle latitudes, 92nd orbit; d) radiating power of ground quartz (laboratory measurements); e) spectrum of the earth's outgoing radiation (Sahara Desert, data from "Nimbus 4" weather satellite). The dashed curves indicate black-body radiation at the corresponding temperatures.

The dark regions of Mars (the so-called "seas") are found to average 10°K warmer than the light areas ("continents"). This is explained by the fact that the dark regions have lower albedos than the light ones.

Unlike the South Polar cap, which disappears in summer, the North Polar cap exists year-round, and it is therefore possible that the total amount of solid carbon dioxide and the water frozen into it considerably exceeds the quantity of these substances in the Martian atmosphere.

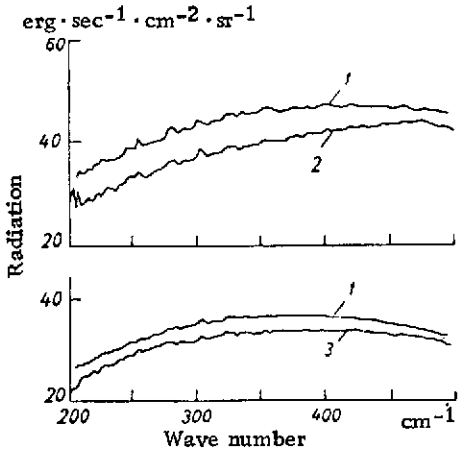

Figure 3. Water Vapor Rotational Spectra of the Martian Atmosphere as Recorded Above South Polar Cap. 1) Calculated ("synthesized") spectra obtained for 10-μm water-vapor content; 2, 3) measured spectra (30th and 116th orbits, respectively). The calculated spectra have been shifted vertically away from the measured spectra for convenience of comparison (they actually coincide).

The temperature of the troposphere was determined from remote IR soundings based on the results of spectral measurements of the outgoing thermal radiation in the 15-μm carbon dioxide band [73]. These measurements (a total of more than 20 000 spectra were recorded) indicated that, on the whole, the infrared spectra of the radiation outgoing from Mars are more uniform than the corresponding terrestrial spectra (Fig. 2). There is a sharp difference in the regions of the South and North Polar caps, where the absorption bands are transformed into emission bands (Fig. 2, a, b, and c) by the temperature inversions characteristic for certain polar regions (for further details, see Chapter III). /17

In the 250-500 cm^{-1} band, the spectra are characterized by the rotational structure of the water vapor absorption band (Fig. 2, b and c, and Fig. 3). The

*"Mariner 9" used an IRIS-M interference spectrometer to make measurements in the range from 50 μm (200 cm^{-1}) to 5 μm (2000 cm^{-1}) with a spectral resolution of 2.4 cm^{-1} and a spatial resolution of 125 km [73].

strongest lines at 254, 278, 303, 324, and 328 cm^{-1} were used to determine the water-vapor content. Weak water-vapor lines are observed at wave numbers larger than 1300 cm^{-1}. In the 500-800 cm^{-1} interval, the structure of the spectrum is determined chiefly by carbon dioxide.

Comparison with the calculated spectra indicated that the isotope-concentration ratios $^{12}C/^{13}C$ and $^{16}O/^{18}O$ are approximately the same as on the earth. The broad minimum around 1100 cm^{-1} and the weaker band at 480 cm^{-1} (Fig. 2c) should be ascribed to the dust. The spectra reproduced in Figs. 2c and 2e can be used for comparison of the features of the Martian and terrestrial outgoing-radiation spectra.

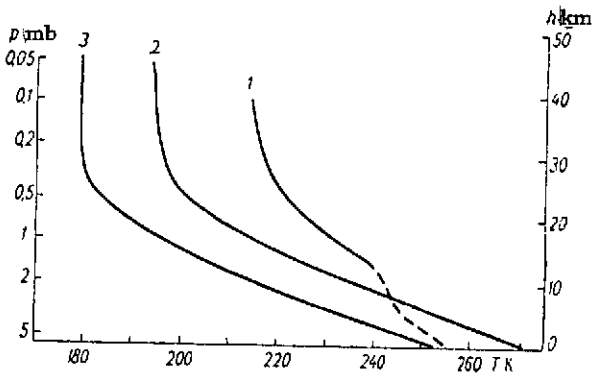

Figure 4. Vertical Temperature Profiles in the Martian Atmosphere at Various Dust Contents. 1) Heavy Dust in Atmosphere (20th Orbit, L_s = 293°); 2) clearing atmosphere (92nd orbit, L_s = 314°); 3) transparent atmosphere (174th orbit, L_s = 336°).

The structural similarity of the spectra in the region of the 15-μm carbon dioxide band indicates that temperature decreases with height in both cases. However, there is an exception in the maximum at 667 cm-1 in the earth's spectrum, which is due to the temperature inversion associated with absorption of solar radiation by ozone. The Martian spectrum lacks the 1042 cm^{-1} ozone band, which is quite distinct in the earth's spectrum, and the spectral structure due to water vapor is much less distinct.

Comparison of the Martian spectrum with the laboratory spectrum of quartz (Fig. 2d) appears to indicate that the characteristic quartz band appears in the 1080-1250 cm-1 region of the Martian spectrum (Fig. 2c).

The results of determination of the vertical temperature profiles at 30°S appear in Fig. 4. We see that a small lapse rate is characteristic for the dust-laden atmosphere. This can be explained by the presence in the planet's atmosphere of dust that absorbs solar radiation strongly and heats the atmosphere (a similar phenomenon is also observed in the pres- /18

ence of an elevated dust concentration in the earth's atmosphere [55]). As the atmosphere clears, the lapse rate increases (but remains below the dry adiabatic rate) and the upper part of the atmosphere is strongly cooled. Analysis of temperature data for various levels revealed a large diurnal variation at heights ranging up to at least 30 km, with strong variation as a function of latitude. Under the conditions of a heavily dust-laden atmosphere, a temperature maximum is observed at 60°S during the late afternoon hours. As the atmosphere clears, the maximum becomes weaker and is shifted toward the equator and earlier times. The amplitude of the diurnal variation ranges from 15 to 30°K and is considerably greater than the values obtained on the basis of theoretical calculations for either the clear or dusty atmosphere (see Chapter II). Measurements in the range in which the dust is most transparent (around 1300 cm^{-1}), which characterize the temperature of the surface, indicate that surface temperature also has a characteristic diurnal variation, but one quite different from that in the free atmosphere. Surface temperature reaches a maximum near the latitude of the subsolar point (7°S) at about 1300 hours both during the dust storm and after clearing of the atmosphere.

According to radiooccultation measurements, temperature decreases with height beginning at about 15 km, at a lapse rate of 2° K/km [12].

Structure of the brightness field near the horizon. "Mariner 9" photometric studies of the darkening of the limb during the dust storm yielded results that differ from those of "Mariner 7" (1969) and indicate the existence of an optically thick atmosphere formed by dust raised from the surface of the planet. The optical thickness of the dusty atmosphere over the visible (elevated) areas of the planet was $\tau \approx 1$. The brightness profiles of the South Polar region (with a diffuse brightness-discontinuity zone at the boundary of the ice-covered surface) indicate $\tau \lesssim 1$ for the entire thickness of the atmosphere. Over other regions of Mars, $\tau \geq 2$. /19

On the whole, a decrease in brightness up to a height of about 40 km is characteristic for the limb structure; it is followed by a region of transparent atmosphere (extending over about 15 km). A distinct haze layer is identified above the 45-60 km level (pressures 0.1-0.01 mb) (Fig. 5, b and d).* The brightness variation at heights below 40 km is governed by the presence of the dust (according to [72], the scale height for the dust is about 8.3 km). On the other hand, a higher,

*According to [77], this layer, which is no more than 2 km thick and situated near the 0.02-mb (55-km) level, can be regarded as an analog of the earth's noctilucent clouds.

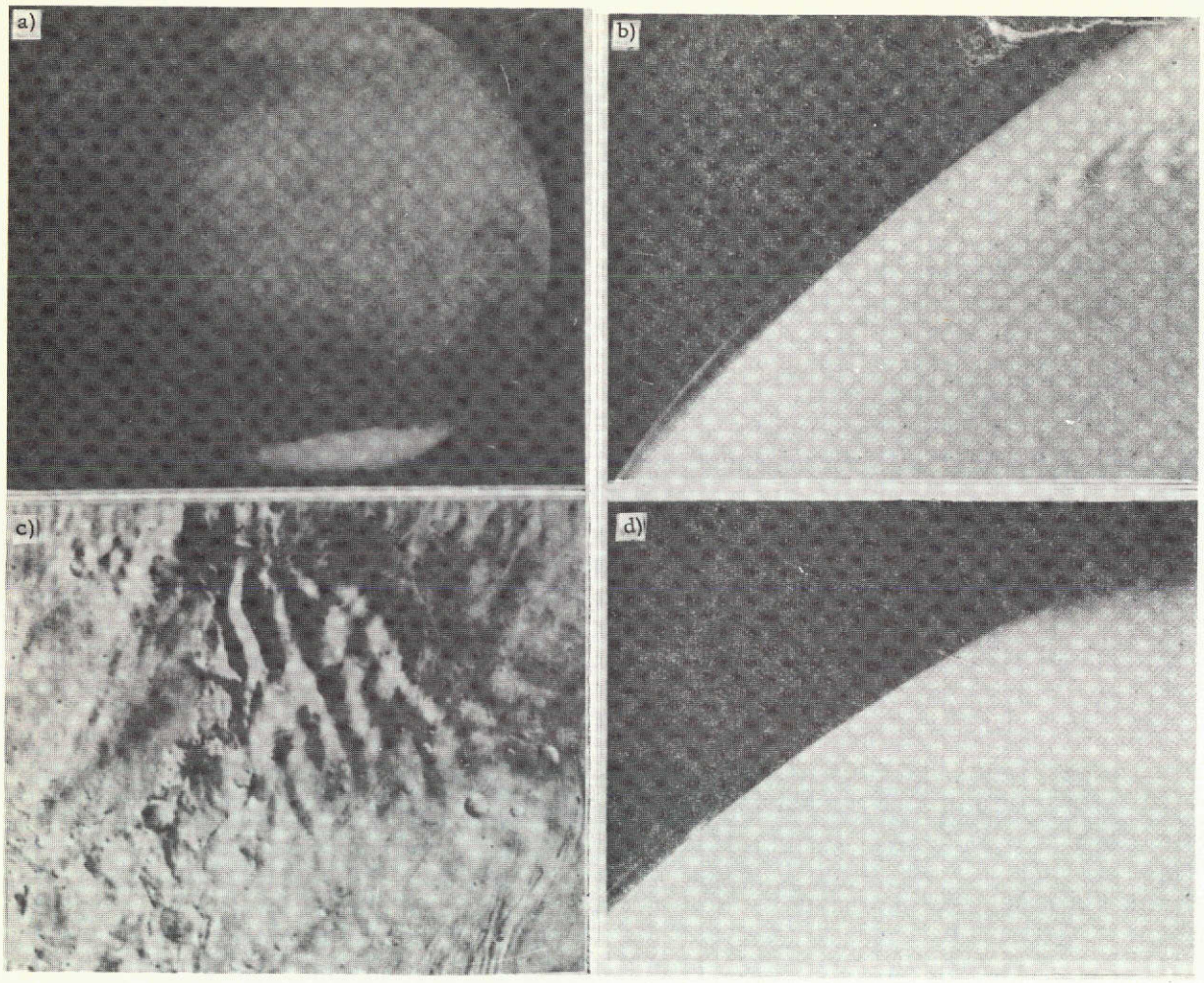

Figure 5. Lee Cloud Waves Formed by Mountain Chain in the Tempe Region According to "Mariner 7" (a) and "Mariner 9" (b, c, d) data. a) Cloud belt visible at eastern margin of polar cap. To the left of it, a cloud appears in the Arcadia region; b) clouds rendered clearly visible by their shadows; the widths of the shadows indicate that the cloud top height is about 20 km (127th orbit); c) the same clouds (195th orbit) on a photograph that clearly illustrates their orographic origin; d) clouds represented as "tufts" near the horizon (at left edge); below them, at a height of about 45 km, a distinctly visible layer of atmospheric haze (see also Fig. b).

bluish layer above 45-60 km is similar to terrestrial haze; this may be a condensate, but its nature is still unknown.

At the terminator, the atmospheric haze is characterized by two kinds of wave structure: 1) waves with $\lambda \sim 40$ km (this is probably the relief of the upper margin of the haze); 2) waves with $\lambda \sim 5$ km (which reflect the presence of vertical structure in the dust layer; see Fig. 5, b and d). Characteristically, elevated areas of the planet are darker than its depressions. The seasonal variation of the planet's brightness may therefore be due to topography and local dust storms.

Dust storms on Mars are highly interesting phenomena. The usually quite transparent Martian atmosphere very quickly becomes just as opaque to visible radiation as the cloudy atmosphere of Venus. Photometric data indicate a transparency increase with increasing wavelength. This indicates a substantial quantity of very fine dust particles with sizes around 1 μm. Earth-based photographic measurements have repeatedly indicated clouds having brightness maxima in the blue and ultraviolet regions of the spectrum [60]. Such clouds must consist of particles much smaller than 1 μm in diameter. The presence of absorbing haze and clouds on Mars should cause cooling of the surface and an increase in atmospheric temperature, and its effects are indeed observed. As we have noted, this enables us to speak of an "antigreenhouse effect," in contrast to the case of Venus, where the atmosphere is heated because of the opacity of the atmosphere in the infrared.

Analysis of "Mariner 9" television data indicated that the Martian atmosphere can, during dust storms, be treated as a model semiinfinite scattering and absorbing layer with a single-scattering albedo of 0.70-0.85 at an effective wavelength of 585 nm [72]. Comparison with the results of approximate theoretical calculations of the brightness angular distribution /20
near the planet's limb lead to the conclusion that the theoretical model is in satisfactory agreement with experiment at an optical thickness of about 3 and a scale height of 8.3 km. Since a single-scattering albedo of 0.7 had also been obtained for the surface of Mars (in the absence of dust storms), we may conclude that the dust-storm particles are raised from the sur- /21
face and that their average size is the same as that of particles of the surface layer of dust. Since it has been established that the surface particles have a size range from 10 to 300 μm, the dust-storm particles evidently have an average radius of at least 10 μm. The dust particles reach heights greater than 30 km during a global dust storm [76].

It appears that surface particles are continuously ejected /22
into the atmosphere during a storm and held suspended there by strong vertical currents. C. Leovy et al. [72] showed that particles with radii up to 30 μm can be held in suspension in the

presence of a vertical velocity on the order of 2 m/sec. In Chapter II we shall discuss in greater detail the physical factors giving rise to the dust storms.

The Martian clouds constitute a phenomenon that is of unquestionable importance in the meteorological regime of the planet (the experience of terrestrial meteorology clearly supports this view). Unfortunately, the available information on the Martian clouds is very incomplete and quite contradictory.

Generally speaking, two categories of Martian clouds are distinguished [67]: 1) clouds that are visible at short wavelengths and gradually become invisible as wavelength increases; 2) clouds that can be observed at long wavelengths but fade out at shorter ones. Of the basic types of clouds – yellow, white, and blue – the latter belong to the former category and the yellow and white clouds to the latter. It is known that the yellow clouds are dust clouds. However, there are no definite data on the composition of the white and blue clouds. The positive polarization of the blue clouds at scattering angles of 0.20° indicates that they consist of much smaller particles than the white clouds, which are negatively polarized in the same range of angles.

Analyzing observational data of the past century on the white clouds, R.A. Wells [67] found that use of polarization phase curves permits almost certain differentiation among white, yellow, and blue clouds, thin layers of atmospheric haze, and deposits of frost on the surface. A new catalog of white clouds containing 252 cases was compiled on the basis of this analysis.

Since observations indicate the predominance of water vapor in the white clouds of the Northern Hemisphere, this can be regarded as an indicator of cloud composition. Comparison of the spectroscopically determined water-vapor contents with the frequency of appearance of white clouds strengthens this conclusion: the higher the water-vapor content, the greater the probability of observing white clouds (the period of the global storm at the end of 1971 is an exception). Another indication of this is found in the fact that white clouds are most frequently observed at the times when the polar caps are smallest in size. "Mariner 9" data indicate the existence of water vapor above the South Polar cap; it is possible that the polar caps are two-layered, consisting of dry and ordinary ice. The aqueous nature of the white clouds is also indicated by the similar latitude curves of water-vapor content and frequency of observation of white clouds. At the same time, it is obvious that we should not expect a constant positive correlation between moisture content and the frequency of occur- /23

rence of the clouds, since other factors may influence cloud formation. On the whole, the data cited testify in favor of the hypothesis that the white clouds are composed of water. The nature of the blue clouds remains unclear. They might be formed above white clouds and consist of dry-ice crystals.

It is noted in [68] that telescopic photographs of Mars in blue light clearly indicate the existence of both diffuse and discrete details against of the background of the planet's relatively dark disk. These bright details have been called both blue and white clouds (actually, their color is nearer white than blue). The nature of these clouds has not yet been established. To avoid confusion, the authors of [68] proposed that both kind of clouds be called white.

Analysis of "Mariner 6" and "Mariner 7" television pictures indicated that discrete white clouds (DWC) are sometimes observed in the Hellas region (Southern Hemisphere), which has no visible (down to scales on the order of 500 m) topographic features, and also in regions with pronounced relief, e.g., Nix Olympica and Elysium (Northern Hemisphere). S.A. Smith and B.A. Smith's detailed analysis [68] of features of the diurnal and seasonal variability of the DWC in these three regions (photographs obtained in the blue and ultraviolet were used as raw material) showed that there is a distinct annual variation of DWC intensity in all three areas – Elysium (22°N), Nix Olympica (18°N), and Hellas (43°S), with a maximum at a solar planetocentric longitude L_s = 110° and a secondary maximum (in the Hellas region) at L_s = 340°. The Elysium and Nix Olympica regions have a diurnal variation of the DWC, with a brightness increase during periods of DWC activity, although the clouds are never observed here during the early morning hours.

It can therefore be assumed that two types of DWC exist. Clouds of the first type are formed during the late morning or early afternoon hours, with a subsequent increase in their brightness extending over several hours (Elysium, Nix Olympica); they have a pronounced diurnal variation and are formed most actively in midsummer. These clouds remain bright even in the zone of the evening terminator, but are not observed in the region of the morning terminator. Clouds of the first type are apparently associated with the dark regions of Mars and probably consist of ice crystals. Clouds of the second type (Hellas) do not exhibit a diurnal variation, are brightest in the middle of winter, and form in the cold regions of Mars. These are most probably not clouds but deposits of dry-ice frost crystals on the Martian surface.

The aqueous nature of clouds of the first type is confirm-

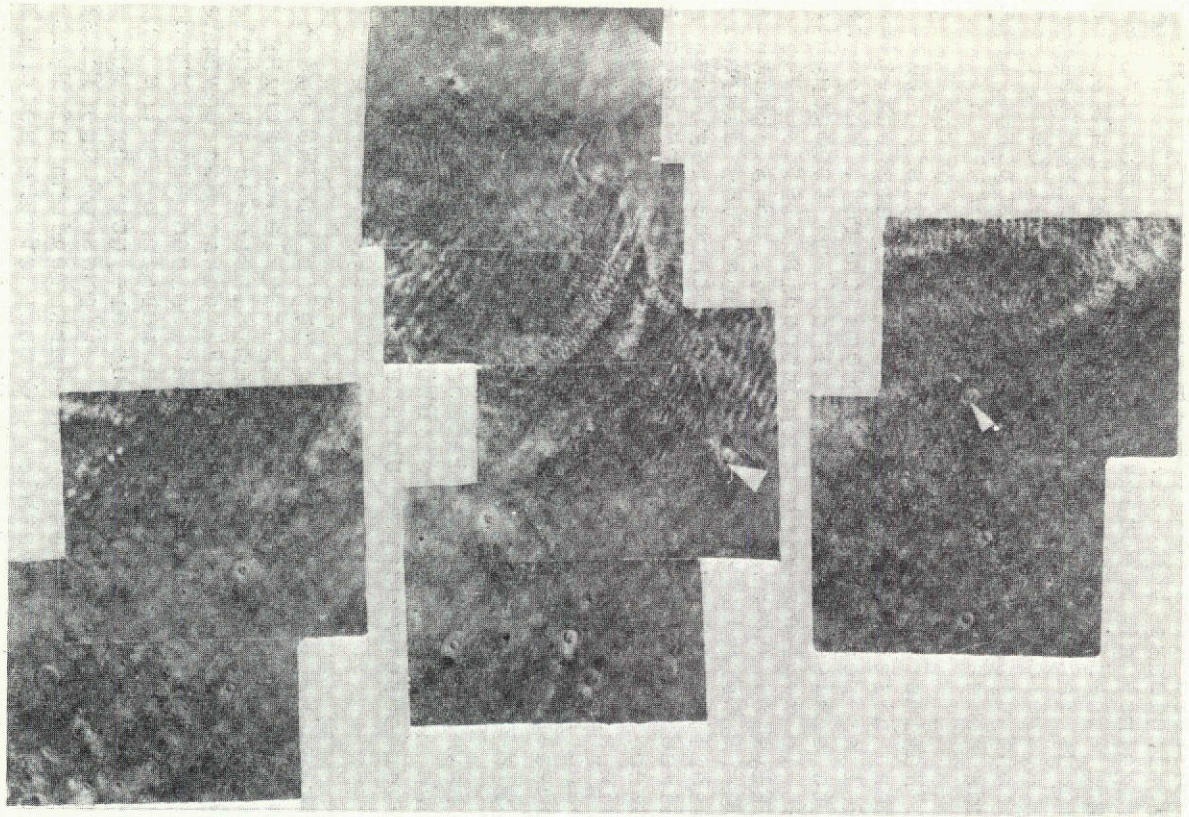

Figure 6. Mosaic of "Mariner 9" Television Pictures Illustrating the Evolution of Wavy-Cloud Systems Near the North Polar "Cap" Over Three Successive Days (203rd, 205th, and 207th Orbits). The crater indicated by the arrow has the coordinates 41°N, 29°W; the distance covered along the vertical by the mosaic at the center is 650 km.

ed by the correlation between the frequency of their occurrence and the content of water vapor in the atmosphere (according to spectroscopic data) in the range of solar longitudes from 0 to 150°. These clouds may be either of orographic origin or due to local outgassing of water vapor from the Martian surface (in this case, the diurnal and annual variations of the clouds are determined by the corresponding variability of the cloud-forming conditions in the atmosphere). /24

A detailed picture of cloud development on Mars emerged from analysis of "Mariner 9" television pictures of the planet [72]. After the global dust storm had subsided and the optical thickness of the atmosphere had dropped to about 0.1, it was found that most of the Martian atmosphere north of 45°N is characterized by variable cloudness — including the polar cap, which should be regarded as an effect of condensation in the atmosphere but not on the surface at this time of year (late winter). The most strongly developed systems include orographic wavelike clouds that form in the zone of westerly transport over surfaces with well-defined nonuniform relief. These extensive cloud systems resemble the baroclinic waves of terrestrial lows in this case. Clouds are also observed over regions with large craters. After the end of the global storm, local dust storms were encountered in a few regions of the planet, apparently due to strong convection generated as a result of strong absorption of solar radiation by the dusty atmosphere. Many of the television pictures transmitted by "Mariner 9" illustrate the above relationships (all of these pictures were obtained using an orange filter, with a corresponding effective wavelength of 610 nm).

Figure 6 presents an interesting picture of the evolution of clouds on three successive days (the central group of pictures is from the 205th orbit). On the first day, we observe only signs of wavelike clouds in the northwestern part of the picture, and diffuse clouds to the northeast. However, even on the next day (on this day, the photographs cover a larger area of Mars), these wavelike clouds are much more distinctly developed. To the north of 45°N, we observe an extensive zone covered by two systems of belts of wavelike clouds (the characteristic distance between belts is about 5 km). The contours, scales, and structure of the cloud belts bear a close resemblance to weather-satellite television pictures of cold-front zones. This impression is strengthened by analysis of the three series of pictures, which indicate that these cloud-belt systems moved at least 500 km toward the southeast in the course of a day and acquired a more latitudinal orientation.

The numerical modeling of the general circulation of the Martian atmosphere that was reported by C. Leovy and Y. Mintz

in [26] indicates the existence of cyclonic activity in northern latitudes at this time of year (see Chapter II). It is most natural to suppose that the wavelike clouds observed on Mars, with their predominant wavelength of about 30 km, are the result /26 of formation of lee gravity waves above a surface width broken relief. This conclusion is confirmed by analysis of the series of television pictures, which indicates the formation of similar local cloud waves in the regions of isolated large craters. The orientation of the waves indicates the predominance of westerly transport in the latitude belt from 45 to 65°N.

It is interesting to note that, contrary to expectation, analysis of the television pictures did not show condensed carbon dioxide to be present on the Martian surface (as in the polar cap, which is clearly observed in the Southern Hemisphere in winter), at least south of 75°N (there are no data for higher latitudes). Only local deposits of "frost" around the rims of crators are observed in the 45-75°N latitude belt.

Figure 6 shows an example of an orographic system of cloud belts that formed under the influence of a mountain chain in the Tempe region. The composition of these clouds still remains unknown. The indirect atmospheric sounding results discussed previously indicate that the surface temperature north of 60°N may be near the condensation point of carbon dioxide. We may accordingly suppose that the polar cap is a low-lying cloud or fog composed of dry ice. In the 45-60°N belt, the surface temperature is not low enough to condense carbon dioxide. Clouds formed at great enough heights may be water, carbon-dioxide, or mixed clouds.

§3. THE UPPER ATMOSPHERE

Because of the large absorption cross-section governed by the electron transitions, much attention is devoted to ultraviolet spectroscopy in study of planetary atmospheres by indirect methods, especially in determining the contents of minor constituents present in amounts smaller than 1 ppm. It is, however, natural that the strong influence of Rayleigh scattering should permit only study of the upper layers of the atmosphere in this case. T. Owen and C. Sagan [12] discussed in detail, for example, the results of an analysis of the ultraviolet spectra of Mars, Jupiter, Saturn, and Venus in the wavelength range 2000-3600 Å (resolution about 25 Å) that were registered by a scanning spectrometer with diffraction grating aboard the Orbiting Astronomical Observatory OAO-A2. The chief purpose of analyzing the data was to establish the possible minor-constituent content ranges in the upper atmospheres of these planets. The method used is quite sensitive for the detection of gases that control absorption, to which an equivalent width of no less than 3 Å corresponds. In all cases,

interpretation of the data was based on the properties of the reflecting layer, since the use of more complex models could hardly be justified. A similar method was also used on the "Mariner" spaceprobes to study the composition of the upper Martian atmosphere. /27

An extensive literature is devoted to the problem of the upper atmosphere of Mars. Here we shall discuss only the results of the most recent experimental studies, with a view chiefly to those aspects of the problem bearing on the interaction between the lower and upper layers. Thus one of the principal problems concerns atmospheric ozone.

Ozone. The great importance of ozone in the earth's atmosphere is common knowledge. Interest in the detection of ozone in the atmosphere of Mars is therefore natural [19-21]. A search for ozone by the ultraviolet spectrometer on "Mariner 7" (1969, end of Martian winter) did not detect its presence anywhere outside of the South Polar cap. The hypothesis was advanced that the gaseous ozone, which absorbs ultraviolet radiation, is adsorbed by solid carbon dioxide on the surface of Mars.

Since the instrument package of "Mariner 9" included a similar instrument (one of the two spectrometer channels covers the range from 2100 to 3500 Å, delivers 15 Å resolution, and records spectra at 3-second intervals), there was interest in checking the earlier results during the early Martian summer and attempting to detect ozone in other regions of the planet. At the spaceprobe's average height of 2300 km, the spectrometer field is about 20 × 20 km. Measurements were made over various areas of Mars under varying conditions of sighting geometry, spaceprobe height, and solar illumination. Because of the intense dust storm that occurred early during the observations, the spectrometer did not "see" the underlying surface over most of the planet's area. In the region of the South Polar cap, however, there was an increase in the signal at wavelengths around 300 Å due to the high albedo of the surface (here the planet's surface was "viewed" through the atmosphere).

During the first stage of the observations, none of the spectra registered between 90°S and 30°N indicated the presence of ozone. As the dust settled and the atmosphere cleared over the South Polar cap, reflectivity increased noticeably, but there were still no signs of ozone, and this situation continued to day 70 (140th orbit), when the atmosphere here had become transparent.

On the 94th orbit, the spaceprobe executed a maneuver that enabled it to make observations north of 30°N. As soon as the spectrometer field crossed this latitude (on the 102nd orbit),

a monotonic increase in reflectivity at 3050 Å with increasing latitude was observed. Analysis of television pictures showed that only in the 45-50°N belt, where the reflected ultraviolet radiation became very strong, was it possible to observe a haze that could be associated with the presence of a "North Polar cap." Calculation of the intensity ratio of the radiations reflected at 47 and 27°N indicates the existence of a marked depression around 2550 Å (Hartley band), and this is the first sign of the existence of ozone ("Mariner 9" data). /28

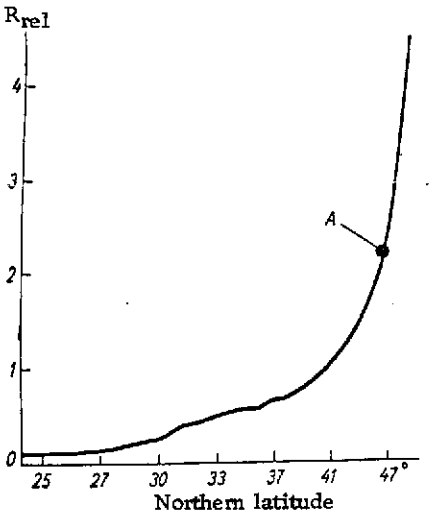

Figure 7. Latitude Dependence of Reflectivity Ratio at 3050 Å Due to Influence of North Polar cap (102nd orbit). The reflected-radiation spectrum corresponding to point A is shown in Fig. 8.

Figure 7 shows the latitude dependence of reflectivity at 3050 Å that results from the presence of the North Polar cap, with the resulting sharp increase in reflection north of 45°N. Figure 8 characterizes the energy distribution in the radiation spectrum reflected at 47°N (point A of Fig. 7) and the spectral curve of the intensity ratio of the radiation reflected at 47 and 27°N. The quite definite depression of the intensity-ratio curve in the range of the Hartley band is beyond question evidence of the presence of ozone.

The depth of this depression increased as it became possible to observe at higher and higher northern latitudes, and on the 144th orbit the absorption by ozone at high latitudes had emerged as very strong (Fig. 8b). From this time on, ozone absorption was consistently observed everywhere north of 30°N, but it was imperceptible in the Southern Hemisphere (including the Polar cap). By the time of the Autumnal Equinox, ozone also appeared in the Southern Hemisphere. By the 200th orbit, ozone was observed everywhere south of 60°S. This permits the conclusion that ozone content has a distinct annual variation on Mars.*

We should note that the aforementioned data on the spectral dependence of the Martian albedo in the ultraviolet – those obtained from OAO-A2 [70] – show no traces of absorption by

*According to [78], the ozone content varies from 3 to 5 μm-atm.

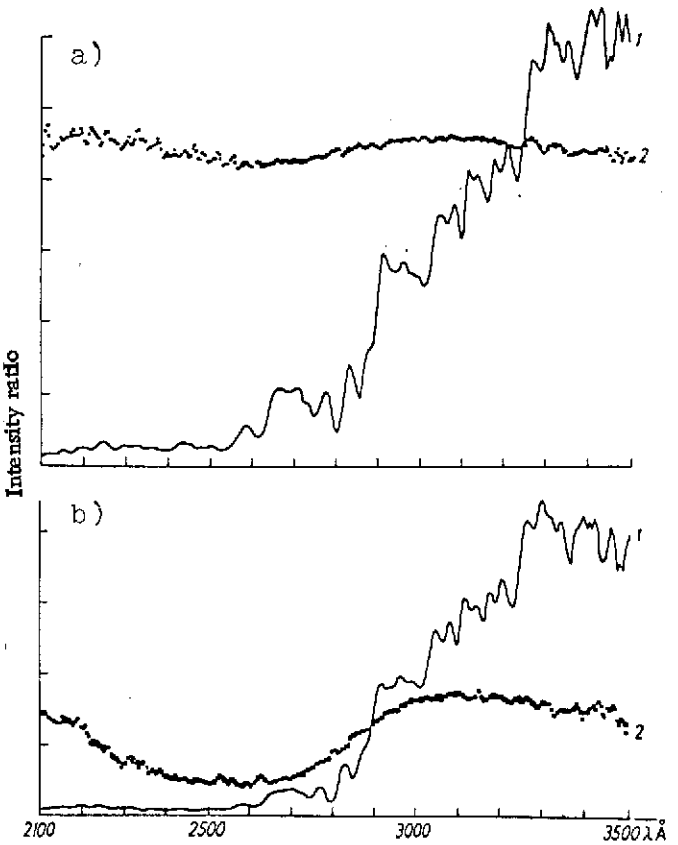

Figure 8. Energy Distribution in Reflected-Radiation Spectrum at 47°N on 102nd Orbit (a) and at 57°N on 144th Orbit (b). 1) Energy distribution; 2) intensity ratios of reflected radiation, 47°N/27°N (a) and 57°N/20°N (b).

minor constituents at all, and are consistent with the pure carbon dioxide model atmosphere with a surface pressure of 5.5 mb or lower (if scattering is also caused by an aerosol component). Since the results considered pertain to the entire disk of the planet, they can neither refute nor confirm the presence of ozone in the Martian atmosphere as observed by the Mariner 6, 7, and 9 spaceprobes.

Theoretical studies carried out for the earth's atmosphere have shown that a "moist" atmosphere should contain less ozone than a "dry" one. It can be supposed that the principal factor /29 determining ozone content in the Martian atmosphere will also be humidity. The decrease in water-vapor content with decreasing temperature favors photochemical processes in which carbon

dioxide and molecular oxygen react to form ozone. It is apparently the variability of water-vapor content that causes the annual ozone variation.

Structure and composition of the upper atmosphere. Spectroscopic measurements of the emission from the upper atmosphere had made it possible to obtain important characteristics of its structural parameters and composition [22-25]. Important data on the structure of the Martian atmosphere have been obtained, for example, on the basis of interpretation of measurements of the Martian ultraviolet radiation in the wavelength range 1900-3400 Å from the spectrometer on "Mariner 9" (28 November to 21 December 1971). Reference [22] discusses the results of 18 series of measurements of the intensity of atmospheric emission near the planet's limb in the Cameron bands of carbon monoxide (1900-2700 Å) and the doublet of the positive carbon dioxide ion (2890 Å). The maximum emission intensities are 200-300 and 50-75 kilorayleighs, respectively. /30

The vertical profile of the emission in the Cameron bands is characterized by an increase in intensity to a maximum at a height of 140 km and an exponential decrease. The intensity at the zenith and the scale height in the zone of the exponential decrease were determined by comparing the measured and "synthetic" profiles. The emission-intensity ratios were found for the CO_2^+ doublet and the Cameron bands.

Since the emission in these bands is governed directly by the absorption of ultraviolet solar radiation and, on the other hand, there is a good correlation between the ultraviolet and 10.7-cm radio emission, the emission intensity at the zenith I_{Cam} can be compared with the radio-emission flux $F_{10.7}$. This type of comparison led to the formula I_{Cam} (in kilorayleighs) = $= 0.062 \times (74 + F_{10.7})$ with a correlation coefficient of 0.80. The average ratio of the emission intensities in the doublet and the Cameron band was found to be 0.24:1. The averaged (over 18 series) scale height is 17.8 km, which corresponds to an exosphere temperature of 325°K. The difference between the maximum and the minimum scale-height values reaches 9.5 km (24.0 – 14.5 km, which corresponds to temperatures of 445°K and 270°K).

Such strong variations of the height scale indicate that the temperature of the upper Martian atmosphere is strongly influenced by processes not directly related to solar activity (for example, heating as a result of dissipation of atmospheric gravity waves and cooling due to turbulence). The results are, in general, in good agreement with the results of theoretical calculations. However, the radio-emission flux

used in the calculations is smaller by at least half than that obtained from determinations of electron density on the basis of radiooccultation measurements.

Study of the first ultraviolet emission spectra of the Martian atmosphere, which were obtained from "Mariner 6" and "Mariner 7," made it possible, thanks to the high quality of the spectra, not only to identify the sources of the emission, but also to understand the mechanism of its excitation. The emission data made it possible to construct models of the vertical distributions of the neutral and ionized components of the upper Martian atmosphere. Starting on 14 November 1971, the ultraviolet spectrometer on "Mariner 9" registered spectra (1100-3500 Å) for 120 days, providing a wealth of material for study of the time variations of the radiation. /31

Analysis of the 1900-3400 Å emission spectrum obtained by averaging over 120 individual spectra pertaining to the height range 100-150 km showed that all emission lines arise directly or indirectly from the action of solar radiation on carbon dioxide. The Cameron bands of carbon monoxide (1900-2700 Å) are strongest; they appear as a result of three processes that govern the dissociation of carbon dioxide (absorption of ultraviolet solar radiation by carbon dioxide is primary to all three). Study of the emission spectra led to the conclusion that ionized carbon dioxide is a secondary component of the Martian atmosphere. The primary component of the ionosphere is ionized molecular oxygen, which is formed as a result of reactions between carbon dioxide and atmospheric oxygen.

Analysis of the spectrum in the 1100-1900 Å band showed the presence of two minor constituents in the atmosphere: atomic hydrogen (1216 Å line)* and atomic oxygen (1304 Å line). It appears that both of these lines are due to resonant scattering of solar radiation. Measurements of the line strength make it possible to determine the vertical concentration profiles of the corresponding atoms. The relative hydrogen concentration at the 135-km level is 10^{-6}%, and that of oxygen 1%. Despite the low concentrations, both of these constituents are important as indicators of and participants in photochemical processes.

Figure 9a shows a model of the composition (neutral components) and structure of the Martian upper atmosphere (height range 100-230 km) constructed from "Mariner 6" and "Mariner 7" ultraviolet emission spectra and radiooccultation measure-

*According to [79], the intensity of the hydrogen emission is 4-5 kilorayleighs.

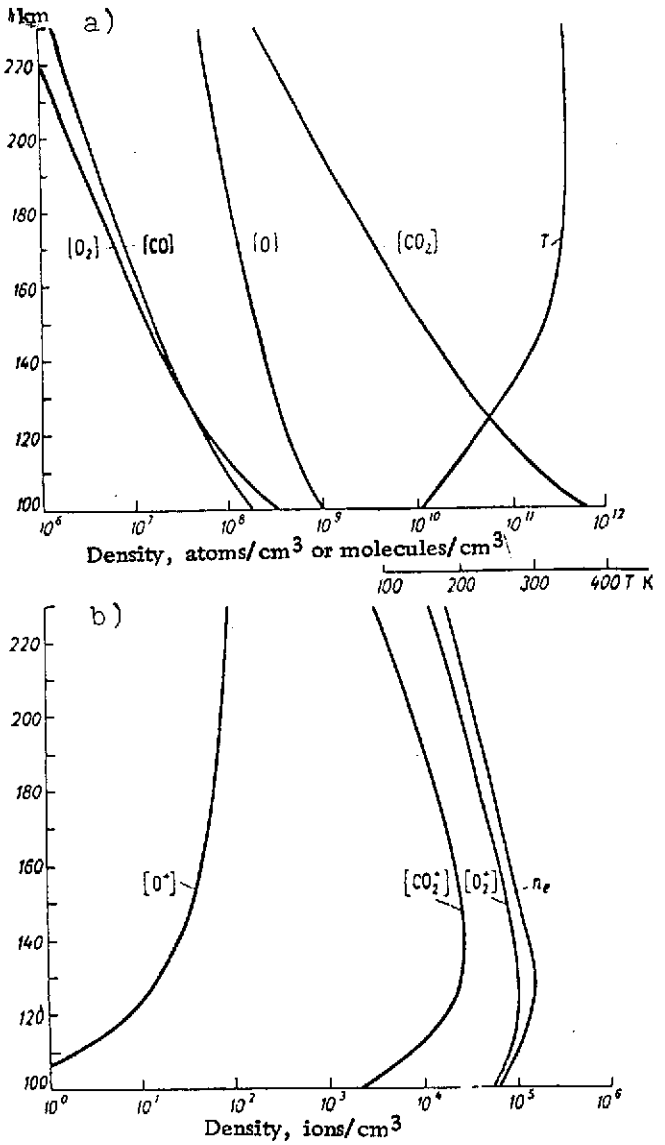

Figure 9. Model of the Composition and Structure of the Martian Atmosphere. a) Model based on use of "Mariner 6" and "Mariner 7" ultraviolet and radiooccultation measurements and results of certain earth-based spectroscopic measurements; b) model of the Martian ionosphere computed using the model shown in Fig. 9a and laboratory measurements of the constants of the ion-atom and ion-molecule reactions.

ments and data from certain earth-based spectroscopic measurements. Figure 9b shows an analogous model of the ionosphere. It was assumed in construction of the models that the level of diffusion separation is at a height of 100 km. The most important factor determining the composition of the ionosphere is the reaction between atomic oxygen and ionized carbon dioxide.*

If it is assumed that the lower boundary of the exosphere is at the 230-km level and the average temperature is 325°K, the flux of hydrogen atoms dissipating into space is $2 \cdot 10^8$ atoms $\times$ $cm^{-2} \cdot sec^{-1}$. If we assume that this flux has prevailed for 4.5 billion years and that the dissociation of water vapor is the sole source of hydrogen, we find that this would require an amount of water equivalent to a 4-meter layer surrounding the planet and that the oxygen content of the Martian atmosphere would have to be $2.5 \cdot 10^4$ times that now observed (it is possible that the oxygen reacted with a substance in the soil or was dissipated by nonthermal mechanisms). What is important here is that, despite the equality of the solar wind flux reaching Mars and the dissipating flux of hydrogen atoms, the solar wind cannot be a source of hydrogen for the Martian atmosphere, since the solar-wind protons are deflected by the induced magnetosphere. /33

Analysis of the emission in the Lyman alpha lines showed that this emission is at a maximum (7.2 kilorayleighs) at a height of about 150 km and that it drops to 2.7 kilorayleighs near the terminator as the spectrometer field crosses the planet's disk; however, the relative variability of the radiation intensity over a period of 120 days was found to be the same in all cases (about 20%). It appears that these variations are due to variations of the hydrogen-atom concentration or of the solar Lyman alpha radiation, or both together. It is interesting that the time variations of the Lyman alpha emission were found to be unexpectedly small, despite the anomalous conditions of the dust storm, which should have shielded the lower layers of the atmosphere from penetration of solar ultraviolet radiation and thereby prevented photodissociation of water vapor and produced substantial variations of the atmospheric temperature field. Thus, there exists some sort of gigantic buffer that maintains an approximately constant influx of hydrogen atoms into the exosphere in the presence of strong variations in the lower atmosphere of Mars.

---

*According to [80], the parameters of the upper atmosphere should have a diurnal variation.

On the basis of contemporary data on the composition of the Martian atmosphere, M.B. McElroy [64] showed that photochemical reactions that lead to the appearance of fast oxygen, carbon, and nitrogen atoms and are responsible for high rates of loss of these atoms from the atmosphere of Mars should play the principal role in the evolution of the atmosphere's composition.

CHAPTER II

/34

THE GENERAL CIRCULATION OF THE ATMOSPHERE ACCORDING TO NUMERICAL MODELING DATA

The most complete numerical modeling of the general circulation of the Martian atmosphere is due to C. Leovy and Y. Mintz [26], who used a so-called two-level model of Mintz and Arakawa's primitive equations for their calculations. The numerical simulation of the atmosphere's general circulation that they undertook was based on integration of the following system of thermohydrodynamic equations (in spherical coordinates):

the equation of horizontal motion

$$\frac{\partial}{\partial t}(\pi \mathbf{V}) = -\nabla(\pi \mathbf{V}\mathbf{V}) - \frac{\partial}{\partial \sigma}(\pi \dot{\sigma} \mathbf{V}) - 2\Omega \sin k\,(\pi \mathbf{V}) - \\ -[\nabla(\pi \Phi) - (\Phi - bRT)\nabla \pi] - \pi \mathbf{F}; \tag{5}$$

the heat-flux equation

$$\frac{\partial}{\partial t}(\pi T) = -\nabla(\pi \mathbf{V} T) - \frac{\partial}{\partial \sigma}(\pi \dot{\sigma} T) - \frac{bRT}{c_p}\frac{dp}{dt} + \frac{\pi}{c_p}\dot{h}; \tag{6}$$

the equation for the pressure tendency

$$\frac{\partial \pi}{\partial t} = -\int_0^1 \nabla(\pi \mathbf{V})\, d\sigma - (\pi \dot{\sigma})\Big|_{\sigma=1}. \tag{7}$$

Here $\pi = (p_S - p_T)$, p_S and p_T are the pressures at the lower and upper boundaries of the atmosphere, $\sigma = \frac{p - p_T}{p_S - p_T}$ is the vertical coordinate, V is the horizontal velocity vector, ∇ is the Laplace operator on the surface of a sphere, Ω is the velocity of the planet's rotation, and Φ is the geopotential, which is defined by

$$\Phi(\sigma) = \int_\sigma^1 bRT\, d\sigma,$$

where R is the gas constant, c_p is the heat capacity at constant pressure, F is the force of friction per unit mass, T is the temperature, k is the vertical unit vector, $b = \left[\sigma + \frac{p_T}{\pi}\right]^{-1}$, $\dot{h}$ /35 is the total heat flux per unit mass, and $\dot{\sigma}$ is the individual derivative determined by the relation

$$\dot{\pi\sigma} = \int_0^\sigma \nabla(\pi \mathbf{V})\, d\sigma - \sigma \frac{\partial \pi}{\partial t}. \tag{8}$$

The individual pressure derivative is determined by the equation

$$\frac{\partial p}{\partial t} = \sigma\left(\frac{\partial \pi}{\partial t} + \mathbf{V}\nabla\pi\right) + \dot{\pi\sigma}. \tag{9}$$

The calculations were made using a spherical grid with steps of 9° in longitude and 7° in latitude. The two-level structure in the vertical direction corresponded to the values $\sigma = 1/4$ and $\sigma = 3/4$, which are equivalent to heights of roughly 12 and 3 km. The pressure at surface level was assumed equal to $p_S = 5$ mb. The level $\sigma = 0$ corresponds to a pressure of 0.415 mb. The calculations were made for a pure carbon dioxide atmosphere. The heat flux was determined with consideration of absorption of solar radiation by the atmosphere and by the surface of the planet (using data obtained by G. de Vaucouleurs [27] for the Martian surface albedo), and also of radiative and convective heat transfer. The latent heat associated with the condensation or sublimation of carbon dioxide on the surface was taken into account.

Transmission functions according to [28] were used in analyzing the transfer of thermal radiation in the atmosphere. The surface temperature needed for calculation of radiative and convective heat transfer was determined from the heat-balance equation

$$(1-A)S - I - P - D + L = 0. \tag{10}$$

Here A is the albedo of the surface, S is the solar radiation flux, I is the effective radiation of the surface, P is the convective heat flux, D is the heat flux in the soil, and L is the heat flux associated with condensation or sublimation of carbon dioxide on the soil.

When the surface temperature drops to the condensation temperature of CO_2 (143.6°K), it is assumed in the calculations that $\frac{\partial T}{\partial t} = 0$ at the surface and that the albedo A assumes a value of 0.6. The initial conditions were those of the isothermal atmosphere at T = 200°K. The subsolar point was placed at longitude 0° and 24.8°S (Southern Hemisphere summer). The initial mass of condensed carbon dioxide was put equal to zero.

Figure 10 shows calculated results for the time variations of the average total kinetic energy K calculated for the entire atmosphere (1), the average disturbance kinetic energy

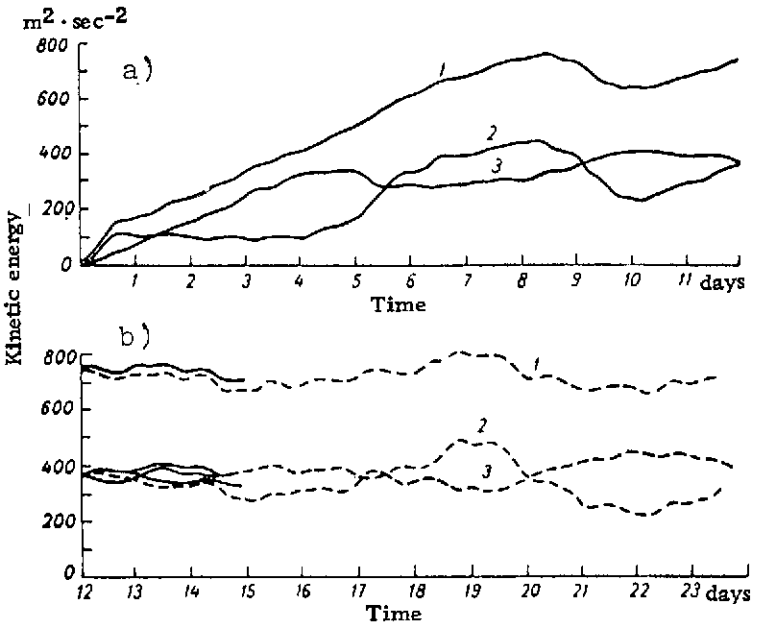

Figure 10. Kinetic Energy as a Function of Time. a) Upper level (T1); b) lower level (T3). 1) Total kinetic energy (K); 2) average disturbance kinetic energy (K'); 3) average zonal kinetic energy ($\overline{K}$).

$K' = K - \overline{K}$ (2), and the average zonal kinetic energy $\overline{K}$ with averaging over longitude (3) (the abscissa is the number of Martian days elapsed from the start of the experiment). As we see, the "acceleration" of the atmosphere (the period of continuously increasing kinetic energy) takes 7-8 Martian days (the length of the day on Mars is 24 hours 37 minutes). Obviously, this low inertia of the Martian atmosphere results from its small (compared to the earth and Venus) mass (see Table 1). The curves of Fig. 10 show very substantial diurnal variations and a six-day periodicity. /36

Figure 11 presents averaged meridional profiles of the zonal (the plus sign corresponds to a westerly wind) and meridional (the plus sign corresponds to a southerly wind) wind-velocity components; the solid and dashed curves characterize the wind profiles at the upper ($\sigma = 1/4$) and lower ($\sigma = 3/4$) levels of the model. These data indicate distinct meridional fluxes in low latitudes, which suggest the existence of a strong meridional circulation with ascending currents in the subtropics of the Southern (summer) Hemisphere and descending currents in the Northern Hemisphere.

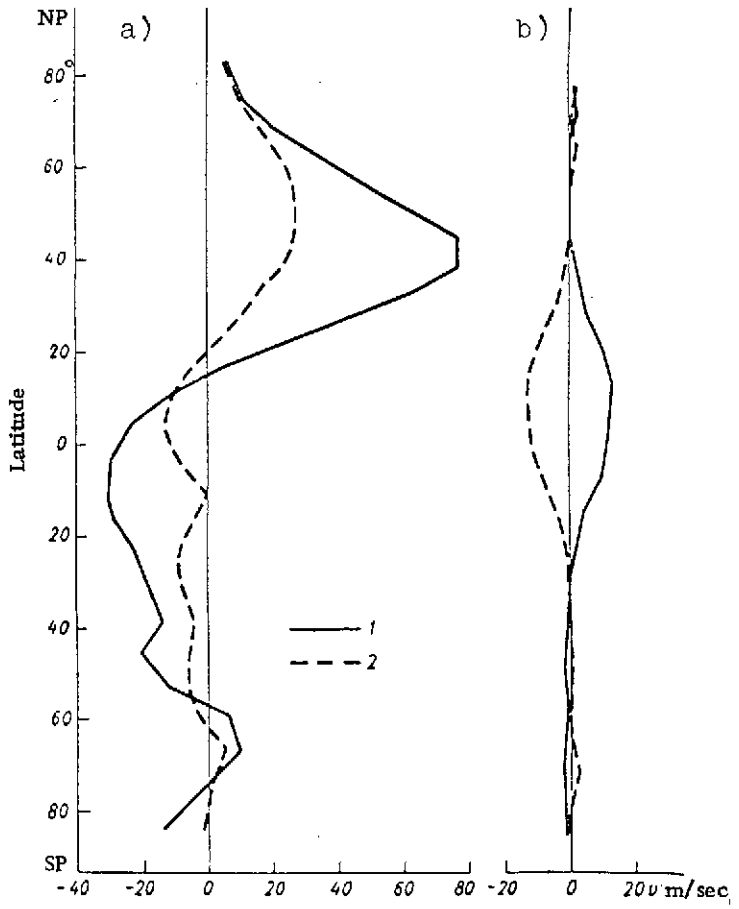

Figure 11. Meridional Profiles of Zonal (a) and Meridional (b) Wind Components. 1) Upper level; 2) lower level.

Westerly winds prevail in middle latitudes of the Northern Hemisphere, with a powerful jet stream at the upper level, while weak easterly winds predominate in the Southern Hemisphere. The data considered correspond to the tenth day of the experiment, when the average zonal kinetic energy reaches a relative maximum. Weakening and broadening of the jet-stream zone are characteristic for the 14th day, when the kinetic energy is at a relative minimum. Similar variations also occur at the same phases of the kinetic-energy variation. /37

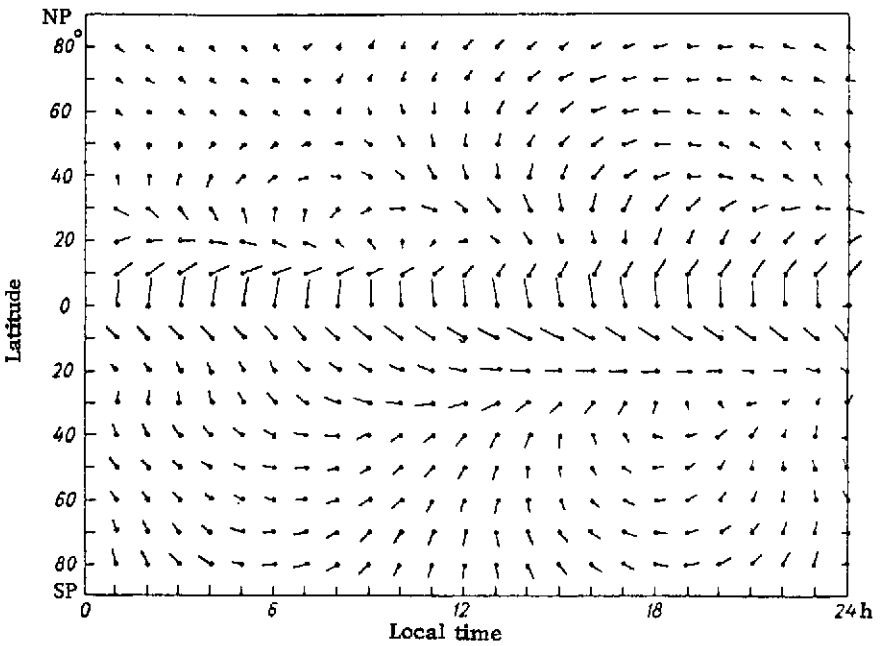

Figure 12. Wind Field at Height of 10 km, Calculated from Measured Temperature Field. The absolute value of the wind vector, which equals the distance between points, corresponds to a wind velocity of 50 m/sec.

R. Hanel et al. [73] made an attempt at approximate calculation of the wind field at mean level (10 km) on the basis of the measured temperature field.* Figure 12 shows the results obtained using temperature data averaged over the period of the 1st through 85th orbits (results pertaining to low latitudes, where the Coriolis force does not make itself felt, are very unreliable). The most important feature of the wind field is the strong diurnal-tide component. A comparison with data calculated in the geostrophic approximation showed that the latter is totally unsatisfactory under the conditions of Mars. The data in Fig. 13 and 14 can be compared to appraise the realism of the numerical-modeling results; substantial disagreements are indicated. /38

Figure 13 shows meridional average surface and atmospheric temperature profiles for the 14th day of the experiment (curves 1). Also shown for comparison are the average-temperature profiles (curves 2) obtained without consideration of circulation (model of radiative-convective equilibrium). We see that

*A more detailed analysis of this problem will be found in [81].

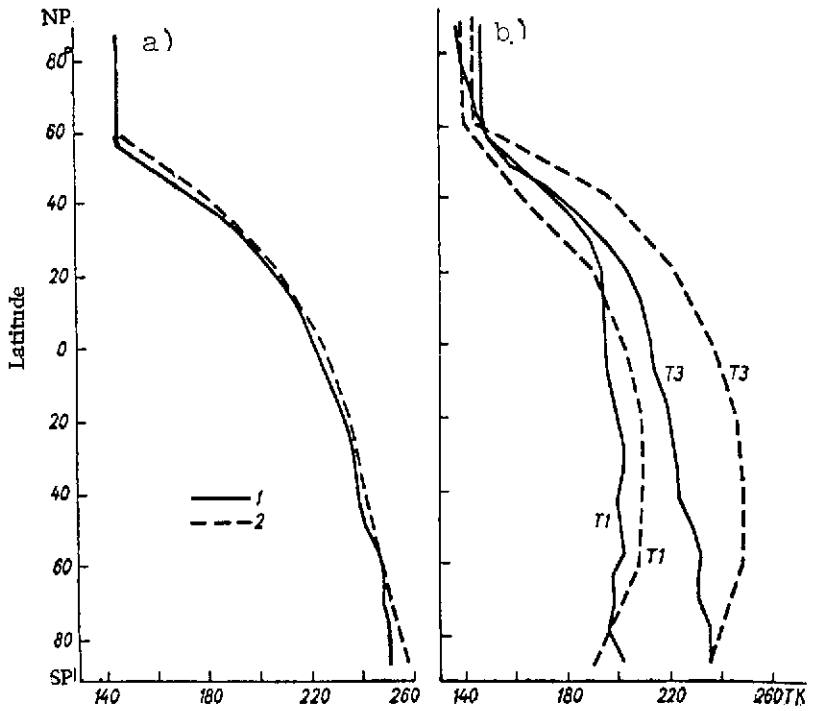

Figure 13. Meridional Profiles of Averaged Surface (a) and Atmospheric (b) Temperatures for the 14th Day of the Experiment. 1) With consideration of circulation; 2) without consideration of circulation.

surface temperature depends little on features of the circulation. However, the temperature of the atmosphere varies appreciably when circulation is taken into account. Circulation also has a marked influence on the latitudinal temperature gradients. Stone [63] proposed a simplified approach to investigation of the general circulation of planetary atmospheres based on the assumption that the radiant heat flux is balanced by the heat fluxes due to turbulence, convection, and the potential energy governed by large-scale vortices.* /39

The straight vertical segments of the meridional temperature profile at high latitudes in the Northen (winter) Hemi-

*An approximate solution of the problem of the global circulation characteristics of planetary atmospheres was proposed in [56].

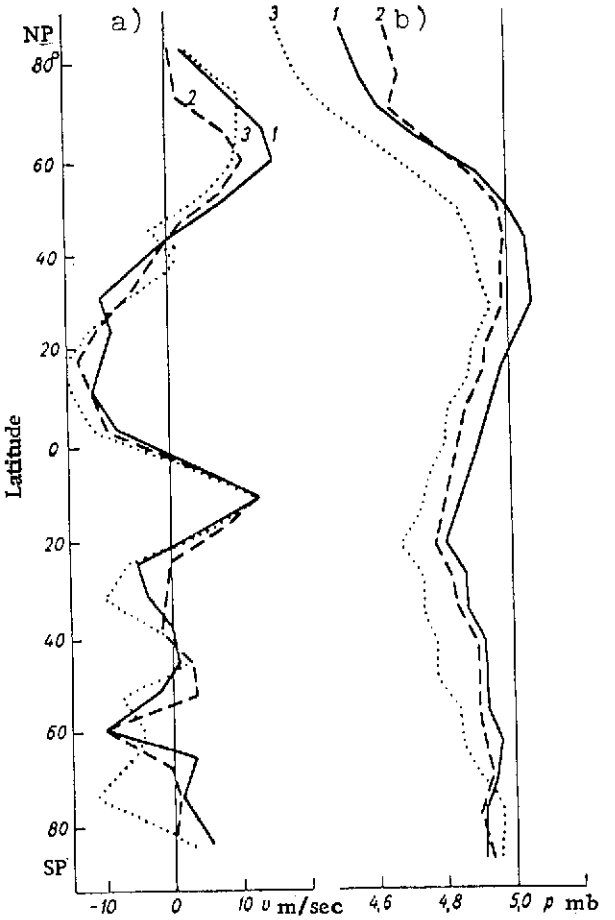

Figure 14. Meridional Profiles of Latitude-Averaged Wind Velocity (a) and Pressure (b). Curves 1, 2, and 3 correspond to 10th, 14th, and 22nd days of the experiment.

sphere indicate the development of a polar cap consisting of solid carbon dioxide. In numerical modeling, this cap appeared on the second day and had stabilized by the sixth day. Its width is consistent with the maximum observed width [29] and, as is shown by a comparison with C. Leovy's data [61], depends little on atmospheric circulation. The air temperature over the polar cap does not drop far below the condensation point of CO_2 despite radiative cooling of the atmosphere — a result of "warming" by the planetary circulation. /40

Figure 14 shows meridional profiles of the latitude-aver-

aged wind velocity (a) and pressure (b) at the surface for the 10th, 14th, and 22nd days of the experiment. Features shown /41
are a pressure minimum at the subsolar point, a band of maximum pressure in the region of 35°N, and an extensive low-pressure center in the region of the North Pole, the latter associated with the formation of the polar ice cap. The average rate of pressure decrease during formation of the polar cap is 0.01 mb/day.

Although the zonal "surface" wind is not exactly geostrophic, there is a tendency to geostrophicity. The most significant features of the meridional wind profile are westerly transport in high latitudes and easterly flows in low latitudes of the winter hemisphere, a narrow belt of westerlies in the tropics, and prevailing easterly flows in the Southern Hemisphere.

Calculation of the planetary temperature fields at various times showed that a "wave" circulation resembling that of the earth gradually forms at the upper level in the temperature field in middle northern latitudes. At early stages in this development, long waves (with a wave number of four) are displaced easterward at velocities from 15 to 30 m/sec, but, having reached full development, they become stable and in certain cases begin to move in the opposite direction. A wave number of three becomes most characteristic at late stages in the development.

In the winter hemisphere, there is close agreement between the temperature and wind fields at the upper level, while the summer hemisphere is characterized by the prevalence of diurnal tides with a very sharp reversal of the wind field at 12-hour intervals. The diurnal tides also determine the basic features of the wind and pressure fields near the surface.

Numerical modeling of the general circulation of the Martian atmosphere indicates the existence of pronounced diurnal temperature and kinetic-energy variations. An interesting feature of the circulation on Mars is the strong influence of the diurnal tides. Also very important and consistent with experiment is the conclusion as to the possible formation and parameters of a solid-carbon-dioxide winter polar cap.

A substantial deficiency of the circulation calculations considered above is their neglect of the effects of different types of clouds: clouds composed of CO_2, water vapor, and dust. The dust clouds formed during dust storms on Mars may have a particularly strong influence on the general circulation of the planet.*

*It is also necessary to take the topography into consideration [82].

Since the first data on the vertical temperature profiles, which had been obtained by transmitting radio waves through the Martian atmosphere from the "Mariner 6" and "Mariner 7" space-probes, differed substantially from the results of calculations for the pure carbon dioxide radiation-convection model of the atmosphere (the measurements yielded higher temperatures and a much smaller lapse rate), P.J. Gierasch and R.M. Goody [30] undertook calculations with allowance for the influence of dust in the atmosphere. /42

Although subsequent improvement of the procedure for interpretation of the radiooccultation measurements eliminated the above deficiences almost completely, this did not exclude the urgent need to consider the effects of the dust, as became especially clear on analysis of the "Mariner 9" data obtained during the dust storm, which indicated a high atmospheric temperature (240°K) together with a very slight variation of temperature with height.

Gierasch and Goody showed that allowance for the absorption of solar radiation by dust mixed uniformly with the atmosphere on the assumption that the absorption coefficient is independent of wavelength and that the optical thickness equals 0.1 (approximately 10% of the solar radiation is absorbed by the atmosphere) results in satisfactory agreement between theory and experiment. In contrast to the data for the pure carbon dioxide atmosphere, practically no convective boundary layer is observed in the presence of dust (only for a small part of the day is there a layer of weak convection). The temperature is near 240°K over two scale heights, indicating great stability of the atmosphere. The amplitude of the diurnal temperature variation at heights exceeding 2-3 km is approximately three times that for the case of the pure carbon dioxide atmosphere.

Since heating of the Martian atmosphere by dust absorption of solar radiation may be a quite typical phenomenon, it may cause a whole series of radical changes in our conception of the Martian atmosphere: 1) the high stability would influence motions on all scales; 2) an increase in the amplitude of the diurnal temperature variation would intensify the effects of tidal phenomena; 3) the absence of strong convection would greatly change the nature of the atmosphere's general circulation; 4) the change in turbulent mixing intensity in the troposphere and the increased importance of atmospheric tides could seriously influence the course of photochemical processes in the ionosphere and the height of the turbopause; 5) the possible effects of nonlinear interaction of the dust, radiation, and atmospheric motions would become especially interesting; they might, for example, cause an "explosive" growth of dust clouds under the influence of the force of the horizontal

pressure gradient that arises on the appearance of a local dust cloud (the processes in the Martian atmosphere at the end of 1971 were precisely of this nature).

In summarizing the results from numerical modeling of the general circulation of the Martian atmosphere, we should note that the very first attempts made in this direction yielded encouraging results that agree satisfactorily with experiment. A more complete description of the laws governing the Martian general circulation is next in order.

CHAPTER III

/43

THE OUTGOING RADIATION

The problem of the outgoing radiation field is an important component of research in planetary meteorology. The importance of this problem is determined primarily by the fact that if we know the outgoing radiation fluxes, we can study the relationships in the thermal (radiation) budgets of the planets. Information on the outgoing radiation is also important for understanding of the structural features and compositions of planetary atmospheres.

§1. THE OUTGOING THERMAL RADIATION FIELD AND THE RADIATION BUDGET

In [31-33], we performed numerical modeling experiments with the Martian thermal-radiation field. As has already been noted, the carbon-dioxide Martian atmosphere is similar in many respects to the above-clouds atmosphere of Venus. However, the pressure at the surface of Mars is almost two orders lower than the pressure at cloud-top level on Venus. We may therefore expect the basic features of infrared radiation transfer in the upper Venusian atmosphere to be typical for Mars as well, although the contribution of the atmosphere to formation of the outgoing radiation will be somewhat smaller than that of the surface.

The spectral intensity distribution of the radiation outgoing from Mars was calculated for the eight different stratifications represented in Fig. 15 [34]. It should be noted that unlike the temperature stratifications that are typical for Venus, most of the Martian temperature profiles are characterized by temperature inversions. The only exceptions are profiles I and III, which correspond to the typical outgoing-radiation spectral-intensity curves (Fig. 16) for the carbon dioxide atmosphere with its strong 15-μm carbon dioxide band. The spectral variation of the outgoing radiation for the other temperature stratifications indicates a strong influence of the inversion on the shaping of the outgoing radiation field. The inversion corresponding to stratification VII is so strong that the 15-μm absorption band is transformed into an emission band. The inversion criteria are not as obvious for the remaining /44
stratifications. This is because the temperature peaks of these inversions are situated at heights lower than that of the effective radiating layer, in the range of maximum absorption ($z_e \approx 20$-30 km). Therefore the inversion influences only the wings of the absorption band, for which the effective tempera-

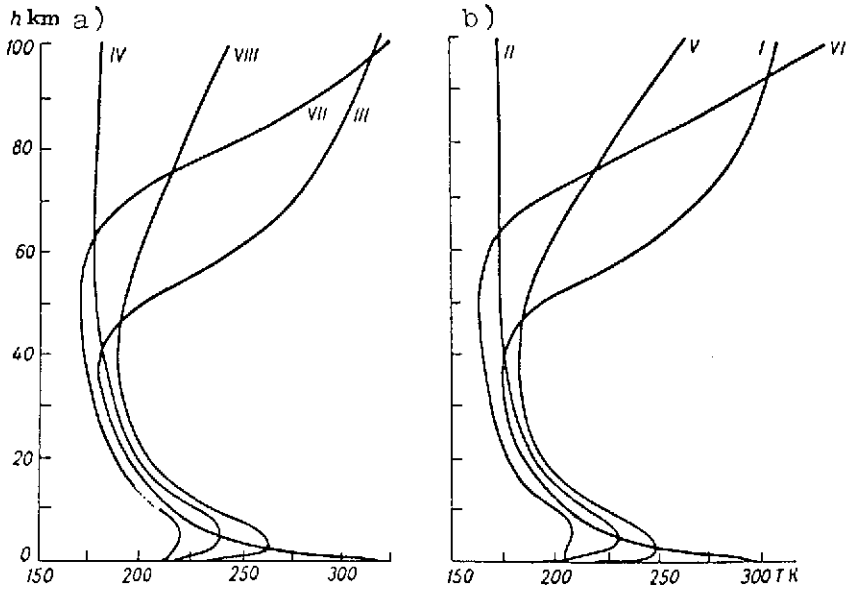

Figure 15. Vertical Profiles of Temperature in the Atmosphere of Mars as Used to Calculate the Outgoing Radiation. a) For the dark side of the planet (latitude −8°); b) for the sunlit side of the planet (latitude +8°). I, III) stratifications at noon; II, IV) at midnight; V, VIII) at sunset; VI, VII) at sunrise.

ture of the radiating layer is found to be higher than that at the center of the band. The range of moderate absorption at $\lambda \approx 13$ μm, in which the spectral maxima for stratifications II, V, and VII are observed, is characteristic from this standpoint. As was noted in Chapter I, it is this behavior of the spectrum with partial "inversion" of the wings of the 15-μm CO_2 absorption band that is characteristic for the "Mariner 9" measured spectra of the dust-free Martian atmosphere.

TABLE 3. SPACE-TIME INTENSITY VARIATIONS OF OUTGOING RADIATION (5-20 μm)

Stratification	Latitude	Time of day	T(0) K	I_{5-20}, W/(m²·sr)			
				θ = 0°	θ = 75°	θ = 80°	θ = 85°
II	+8°	Midnight	195	12,3	12,3	0,88	0,044
V	+8°	Sunset	217	21,1	20,9	2,82	2,14
III	−8°	Noon	310	103,0	99,1	11,10	10,10
VIII	−8°	Sunset	210	20,1	20,8	2,87	1,31

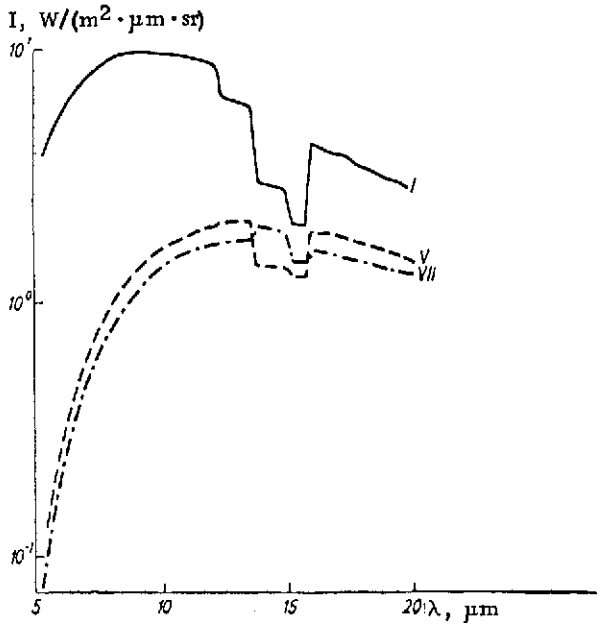

Figure 16. Outgoing Thermal Radiation Spectrum of Mars for Various Temperature Stratifications, as Calculated Using Transmission Function According to Hanel [35].

In our calculations, use of the model proposed by E. Bartko and R.A. Hanel [35] for transmission functions obtained with low and medium spectral resolution made it possible to evaluate the most significant physical effects and relationships and to save machine time. Needless to say, when study of the fine structure of the emission spectrum acquires basic importance (for example, in the problem of the role of small impurities), it is necessary to use transmission functions obtained with high resolution. For this reason, we also made the /45 calculation for a whole series of spectral intervals using the higher-resolution transmission functions obtained in [36] (Fig. 17). Similar calculations had been performed previously by H.-J. Bolle [65] for narrow spectral intervals around the wavelengths 10.4 and 15 μm.

Table 3 shows the variations of outgoing-radiation intensity at 5-20 μm in space and time for various atmospheric /46 stratifications, as obtained from the results of our calculations (θ is the nadir angle).

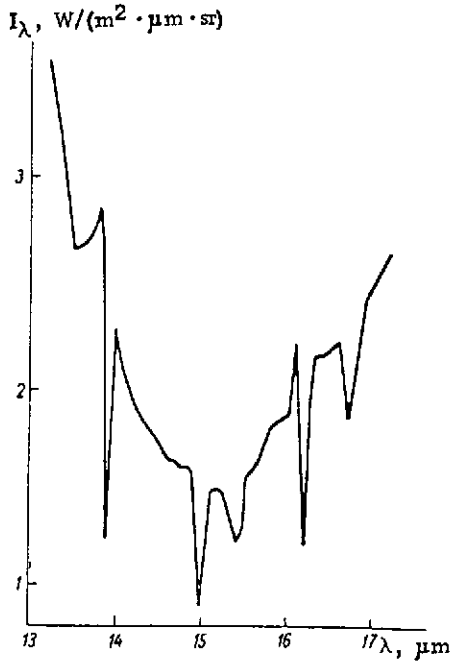

Figure 17. Outgoing Thermal Radiation Spectrum of Mars for the Range of Strong Absorption (15-μm CO_2) Calculated Using Distribution Function According to [36].

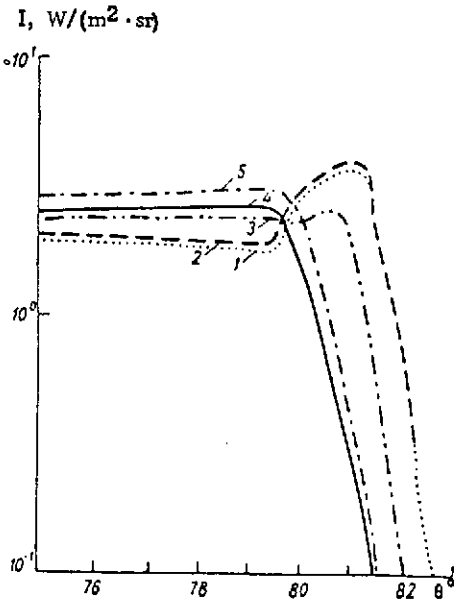

Figure 18. Angular Distribution of Outgoing Radiation Intensity at 10-20 μm for Various Atmospheric Stratifications. 1) IV; 2) VIII; 3) VI; 4) I; 5) III.

The observed spectral features of the variations of the Martian outgoing radiation intensity indicate that, despite its small optical thickness, the atmosphere of Mars makes a substantial contribution to the outgoing radiation (like the above-clouds atmosphere of Venus). This is also indicated by special calculations of the surface contribution to the outgoing radiation. Inferences can also be drawn as to this contribution from the fact that all of the outgoing radiation is shaped by the atmosphere and not by the surface of the planet in the region of the CO_2 absorption band (11-20 μm).

Figure 18 shows the angular distribution of outgoing radiation intensity in the 10-20-μm wavelength interval. We see that the dependence on angle is quite weak in the "subcritical" range of nadir angles ($\theta < \theta_{cr}$, where θ_{cr} corresponds to the planet's limb). On the whole, the nature of the angular variation of the Martian outgoing radiation differs little from the angular trend characteristic of the Venusian atmosphere [31]. With the transition to "transcritical" angles ($\theta > \theta_{cr}$),

we observe the same behavior as in the Venusian atmosphere: there is a brightening effect (an increase in radiation intensities) near the limb.

Let us consider the features of the radiation (thermal) budget of Mars. For the planet as a whole, the flux of absorbed solar radiation must be equal to the outgoing radiation flux:

$$\Phi^{\downarrow} = \Phi^{\uparrow}, \tag{11}$$

TABLE 4. COMPONENTS OF THE RADIATION BUDGET OF MARS

Stratification	$\Phi^{\uparrow}{}^{(1)}$ W/m^2	$\Phi^{\uparrow}{}^{(2)}$ W/m^2	$\Phi^{\uparrow}$ W/m^2	$T_e^{(1)}$ K	$T_e^{(2)}$ K
V	103,04	97,13	116,70	219,5	215,9
I	207,16	165,38	232,92	310,1	279,7

The total amount of solar energy absorbed by Mars per unit of time equals

$$W = q_0(1-A)\pi R^2, \tag{12}$$

where q_0 is the solar constant for Mars, A is its albedo, and R is its radius (see Table 1). Thus the average amount of solar energy absorbed by a unit area of the planet, i.e., the flux $\Phi^{\downarrow}$, is /47

$$\Phi^{\downarrow} = \frac{W}{4\pi R^2} = \frac{q_0}{4}(1-A). \tag{13}$$

The outgoing radiation flux is related to the radiation intensity $I_\lambda(\theta)$:

$$\Phi^{\uparrow} = \int d\lambda \int I_\lambda(\theta)\cos\theta\sin\theta\, d\theta\, d\varphi, \tag{14}$$

where the integration with respect to the angles is carried out over the surface of a sphere, and the wavelength integration from 0 to ∞ (in practice, the range from 1.5 to 50 μm is sufficient). The calculated results for various models of the transmission functions and temperature stratifications appear in Table 4 (for the two extreme models). The last two columns of the tables give the effective temperatures of Mars that correspond to the computed fluxes:

$$T_e = \left(\frac{\Phi^{\uparrow}}{\sigma}\right)^{1/4}, \tag{15}$$

where $\sigma = 5.67 \cdot 10^{-8}$ W/(m$^2 \cdot$K^4) is the Stefan-Boltzmann constant.

Here $\Phi^{\uparrow(1)}$ and $\Phi^{\uparrow(2)}$ are the outgoing-radiation values calculated using the transmission functions of [35] and [36], respectively, $\Phi^{\uparrow}$ is the outgoing radiation due solely to radiation from the underlying surface that passes through the atmosphere (in this case the atmosphere's intrinsic thermal radiation is left out of account), and $T_e^{(1)}$ and $T_e^{(2)}$ are the effective temperatures corresponding to $\Phi^{\uparrow(1)}$ and $\Phi^{\uparrow(2)}$. /48

Stratification V satisfies the radiation-balance condition for the planet within the limits of accuracy of Mars-albedo measurements.

In the former case (stratification V), the effective temperature is below the underlying-surface temperature corresponding to the selected stratification and is a sign of a possible greenhouse effect. Much of the radiation from the surface is absorbed by the atmosphere, and the outgoing radiation is shaped in many regions of the spectrum in the higher and less heated layers of the atmosphere. The small difference between T_e and T_0 in the case of stratification V is associated in this case with the presence of a strong temperature inversion: although the radiation is, as before, shaped in higher layers of the atmosphere, these layers are warmer (because of the inversion).

We see from Table 4 that the difference in the transmission functions has comparatively little effect on the amounts of outgoing radiation $\Phi^{\uparrow}$. The stratification of the atmosphere exerts a much stronger influence.

The above features of the spectral distribution of the Martian outgoing thermal radiation indicate the possibility of estimating temperature profiles by analysis of measured outgoing-radiation spectra. If the transmission functions are not known reliably enough, data on the integral radiation fluxes should be used. But if the transmission functions are adequate, analysis of the spectral trend of the outgoing radiation (especially in the absorption bands) permits more detailed specification of the temperature profiles.

§2. DATA ON THE STRUCTURE OF THE ATMOSPHERE OBTAINED FROM THE RADIATION FIELD

The "Mariner 9" infrared-spectroscopy experiments opened the way to remote sounding of the Martian atmosphere. In this context, it is interesting to compare outgoing thermal radia-

tion spectra obtained from "Mariner 9" data [37, 73] with the calculated spectra and inspect them for features of the vertical temperature profile.

Analysis of calculated Martian outgoing radiation spectra permits the following inferences [31, 33]:

1. In much of the infrared (λ = 3-50 μm), the Martian atmosphere absorbs practically all of the radiation from the underlying surface (the only exceptions are the narrow "transparency windows" at $\lambda \approx$ 6-8 μm and λ = 11 μm). Herein lies one of the basic differences between the strongly absorbing pure carbon dioxide (total CO_2 content in a vertical column $U_t \approx 10^4$ cm·atm) atmosphere of Mars and the earth's atmosphere (the Martian infrared spectra are, on the whole, more uniform than those of the earth). As a result, the outgoing thermal-radiation spectrum is found to depend strongly on features of the vertical temperature distribution. /49

2. In the region of strong absorption, the shape of the outgoing-radiation spectrum is determined by the height of the effective radiating layer z_e and depends strongly on the behavior of the lapse rate. Specifically, "inversion" of the absorption spectrum is possible in the real atmosphere of Mars due to the presence of the temperature inversion in that atmosphere.

3. "Brightening" toward the limb of the planet may be observed in absorption bands as another effect of temperature inversions.

The conclusions given above can be verified with reference to recently published "Mariner 9" measurements of the outgoing radiation spectrum.

As we know, a severe dust storm was observed during these measurements. According to earth-based measurements in the range around λ = 10.5 μm, the infrared-opaque dust cloud rose to a height of about 11 km [38]. The planet's atmosphere remained clearest in the region of the South Polar cap. Measurements made with the IRIS-M IR interference spectrometer on "Mariner 9" appear in Figs. 2 and 3. As we have already noted, the 15-μm CO_2 absorption band appears clearly here either as an emission minimum (Fig. 2c), as is typical for absorbing carbon dioxide atmospheres without temperature inversions, or as a maximum (see Figs. 2a and b), reflecting the presence of inversions. We had obtained a similar type of spectrum (with an emission minimum corresponding to the transmission-function minimum) for a series of temperature profiles in [31, 32] (see

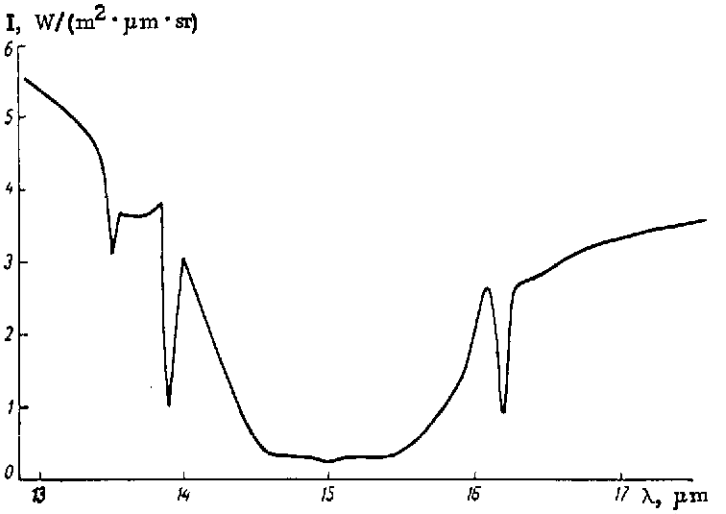

Figure 19. Outgoing Thermal Radiation Spectrum of Mars as Calculated with High-Resolution Transmission Function According to [40].

curve I in Fig. 16). Needless to say, the wavelength-averaged (stepped) transmission functions used in these studies could not have reproduced all details of the observed spectrum. Use of the more detailed transmission functions obtained by V.G. Kunde [39] from the data of R.S. Drayson and C. Young [40] makes possible a more accurate description of the fine structure of the 15-μm CO_2 band in the case of inversion-free temperature profiles [41]. The corresponding calculations are represented in Fig. 19.

The outgoing-radiation spectrum shown in Fig. 2b pertains to the region of the South Polar cap (the lower dashed curve characterizes the radiation from the surface). In this case we observe the situation that is typical for temperature profiles with inversions. We found similar spectral features for such conditions (for example, curve VII in Fig. 16) by calculation in [31]. Since the wings of the absorption band correspond to a value of z_e below the temperature maximum of the inversion, the temperature of the radiating layer is higher in these regions of the spectrum than outside them and we observe a maximum in the emission spectrum. At the center of the absorption band (λ = 15 μm), z_e is above the inflection on the temperature profile, indicating a lower radiating-layer temperature. As a result, the central part of the band does not experience "inversion" (compare Figs. 2a and c). This clearly illustrates the conclusion drawn in [31, 32] to the effect that it is pos- /50

sible to reconstruct details of the temperature profile from the nature of the spectrum in the absorption-band region. In this case, the measured spectrum (Fig. 2, a and b) could not only yield an inference as to the presence of a temperature inversion, but also a height estimate for the temperature maximum based on the "inversion-free" central part of the band and the known variation of $z_e(\lambda)$ within the band.

A temperature-profile reconstruction of this kind was carried out in [42, 73]. The resulting temperature profiles were given in Fig. 4.

PROSPECTS FOR RESEARCH /51

The weather and climate of a planet are determined to a substantial degree by the interaction between its atmosphere and its surface. This interaction takes the form of exchanges of momentum, heat, gases, and radiation. The principal exchange mechanisms are diffusion (molecular and turbulent), convection, and radiation transfer. At present, it is these processes in the Martian atmosphere that have been least thoroughly studied. It is therefore natural that prospects for research in the field of Martian meteorology are primarily dependent on study of the dynamics and transfer of radiation in the boundary layer of the atmosphere. It is especially important to investigate the wind field (both the average values of wind velocity and direction and their fluctuations), the more so since the information now available on the wind has been obtained either by calculation or on the basis of indirect measurement methods.

In view of the above circumstances, considerable interest attaches to the considerations advanced in [43] concerning the meteorological research program proposed for the two lander stages of the "Viking" spaceprobe being built for a 1976 launching to Mars (measurements of wind velocity and direction, atmospheric pressure, temperature, and water-vapor content) with the object of studying the turbulent structure of the atmospheric boundary layer and convective and mesoscale phenomena. The design of this program takes account of peculiarities of the Martian atmosphere, which exhibits not only definite similarities to the earth's atmosphere (influence of Coriolis force, annual variation), but also substantial differences (absence of oceans, low water-vapor content, and absence of a thick cloud cover).

In development of the meteorological instruments, attention has been concentrated on elimination of the effects of the quite large and heated body of the spaceprobe, and appropriate laboratory simulation experiments were carried out for this purpose. It is proposed that the meteorological sensors (except for the pressure sensor) be mounted at the tip of a 3-meter folding boom similar to a second boom designed for soil sampling and biological and chemical studies. The end of the boom can be displaced through 180° in azimuth at a height of about 3 meters, /52 and the length of the boom can be varied. This type of maneuver can be programmed in advance or executed on radio command from the earth. To measure the vertical profiles of the meteorological elements, the boom is displaced vertically to form "platforms" in the height range of interest for periods of several minutes at various times of day. The high-frequency component

of the turbulent temperature and wind fluctuations will also be measured from time to time.

The plans call for specialized measurements of the diurnal variation by determining the averaged values of the meteorological elements over several minutes and repeating such measurements at intervals of approximately forty minutes. To register the passage of dust whirls, thermals, or atmospheric fronts, a command from an automatic controller can increase the frequency of the measurements when the wind velocity exceeds a certain value. Verification of three phenomena predicted by theory is provided for here: 1) the pressure variation due to solar atmospheric tides of large amplitude; 2) wind speed and direction changes of similar nature; 3) the annual variation of pressure (the lander is supposed to function for 90 days). Measurements of the water-vapor content near the Martian surface are highly important. They will be supplemented by simultaneous optical measurements from an orbiting module, which will make it possible to determine the total content of water vapor in a vertical column of atmosphere.

The final choice of sensors for the meteorological measurements has not yet been made. It has been proposed that pressures be measured with various types of manometers in the range 1-30 mb accurate to $\pm$ 0.2 mb, and that temperature be measured with thermocouples or resistance thermometers in the range 130-350°K accurate to $\pm$2°K (in this case, minimization of the radiation error is highly important). A film-type thermal anemometer, which would give errors on the order of 10%, could be used to measure wind velocity. A similar principle is embodied in an instrument for measurement of wind direction accurate to $\pm$ 10-20°. A quartz vibration hygrometer is being studied as a possible humidity sensor. All sensors (except for the one designed to measure humidity) must have time constants of about a second or less.

Because of weight limitations and financial cutbacks, it will probably not be possible to make all of the meteorological measurements described above as originally planned (for example, the movable boom will apparently be shorter and less movable, thus eliminating the possibility of soundings along verticals and strengthening the influence of the spaceprobe's body). However, even a more modest program will be of exceptionally great significance for research in the field of Martian meteorology. This is because of the coordinated quality of the program as a whole and the variety of the information whose acquisition is planned. /53

In addition to the part of the program whose only objective is meteorological research, the 11 experiments planned for the "Viking" include many that are of interest for meteorology but

are broader in scope: 1) measurements of the surface radiation temperature field and the total water-vapor content and acquisition of television pictures of the Martian surface from the orbiting module; 2) "radio occultation" experiments to determine the vertical temperature profile in the troposphere; 3) determination of the temperature and density of the atmosphere from the atmospheric-entry conditions of the lander; 4) measurements of atmospheric composition near the surface and of the properties of the Martian soil.

Problems related to study of the structural parameters and composition of the atmosphere will be solved when "Viking" enters the Martian atmosphere [44]. The range of problems is being determined and the appropriate scientific instrument package is being selected with consideration of the data obtained from Mariners 4, 6, 7, and 9. The basic mission of the "Viking" spaceprobe in this aspect is to perform direct measurements, the results of which are needed to obtain more reliable information on the Martian atmosphere and resolve a number of contradictions in the results obtained by indirect methods during flybys. Contradictions of this nature stem, for example, from the fact that radio-occultation data ("Mariner 4") unexpectedly indicated the existence of a cold lower atmosphere consisting almost exclusively of carbon dioxide and a moderately dense but exceptionally compact ionosphere with a density maximum at 130 km.

The ionosphere measurements produced a "squall" of activity among theoreticians, whose principal purpose was to solve the problem on the basis of an analogy with the earth's atmosphere. The results, however, were contradictory. Resolution of these contradictions requires direct measurements of the vertical O, CO, O_2 and CO_2 concentration profiles in the upper Martian atmosphere, and this is the objective of mass-spectrometer measurements to be made as "Viking" enters the atmosphere. Another important experiment with a bearing on this problem will study the interaction of the solar wind with the Martian upper atmosphere ("erosion" of the atmosphere near the limb of the planet under the action of the solar wind).

Direct density, pressure, and temperature measurements with errors not greater than 5% will be made along the entry trajectory in the lower atmosphere of Mars (at heights from 1.5 to 100 km). These data are needed to investigate the space-time variations of the structural parameters (which determine, among other things, the possibility of formation of haze layers or clouds consisting of condensed carbon dioxide), and can be used to control the results of radiooccultation studies of the atmosphere. /54

There are important meteorological aspects to the meas-

urements to be made with a six-channel IR radiometer designed to produce thermal maps of the planet's surface with the object of studying its thermal inhomogeneities, determining the thermal inertia and spectral emissivity of the soil, and measuring the reflected shortwave radiation [45]. Since the emissivity variations are widest in the wavelength ranges 8-9.5 μm (acid silicates), 9-12 μm (basic silicates), and 5.5-7.2 μm (carbonates), three corresponding channels are provided for measurements with the object of determining the emissivities. The infrared radiation will also be measured in the ranges 18-24 and 24-35 μm. Plans call for measuring brightness temperatures with a resolution of 0.5°K and accuracy better than 1°K. The true temperature of the surface can be found to within a few degrees (as a rule, 2°K) after applying a correction for the emissivity (for certain channels, this correction will amount to 5-10°K).

Thermal-inertia measurements based on the contrasts and time variation of temperature will make it possible to find the thermal conductivity of the soil, since it is the most variable factor (varying through a factor of approximately 50) compared to the other parameters (density and heat capacity) on which soil thermal inertia depends. Simultaneous measurements of albedo in the wavelength range 0.25-3.3 μm are provided to separate the factors determining soil temperature. Thermal inhomogeneities can also be used as indicators of the presence of internal heat sources and "frost" deposits on the surface, and, in the presence of dense clouds, to determine the temperatures and heights at their tops.

The available data (low average dielectric constant, photometric parameters, etc.) indicate that, like the earth and the moon, Mars has a soil-like surface layer. Investigation of the characteristics of this layer is one of the departments of the "Viking" lander program [46]. This problem will be solved on the basis of experience gained in study of the lunar soil. The following data can be used to obtain information on the characteristics of the Martian soil: 1) pictures of the terrain surrounding the lander; 2) dynamic features of the landing; 3) the interaction of the "engine-surface" system during landing; 4) the "behavior" of the soil sampler; 5) thermal measurements; 6) various scientific experiments; 7) radar measurements. It is expected that these data will make it possible to determine the bearing strength of the soil, the cohesion and tenacity of its particles, its internal-friction characteristic, porosity and density, thermal properties, soil particle size distribution, /55 and the inhomogeneity of the soil.

The "Viking" lander mass-spectrometry program provides for study of possible organic compounds in the upper 10-cm layer of the Martian soil and measurement of the majority and minority constituents of the atmosphere (including their isotopic composi-

tion) [47]. Another important objective of the program is to determine the content (and, if possible, the physical state) of the water in the soil and estimate its mineralogical composition from the outgassing products of heated soil samples (limonite and siderite,for example, release characteristic decomposition products at certain temperatures and pressures). The principal purpose of this department of the program is to detect life on Mars. Soluble organic compounds will be analyzed directly by the mass spectrometer or by gas chromatography after fractionation (the compounds will be vaporized at temperatures of 150, 300, and 500°C). The insoluble components will be analyzed from data on their pyrolysis products. The sensitivity of the mass spectrometer, which covers the mass range from 12 to 200, is such that identification is possible even when a hundred compounds are present in a total relative concentration not greater than $5 \cdot 10^{-6}$ (any compound that has a vapor pressure above 10^{-6} Torr at 200°C can be identified at a content by weight on the order of a few nanograms).

Analysis of nine soil samples is planned for study of possible diurnal and seasonal variations. The answer to the question as to the origin and evolution of the Martian atmosphere requires, first of all, measurements of its concentrations of nitrogen and inert gases. Determination of the contents of water vapor and other minor constituents of the atmosphere (oxygen, methane) with a relation to vital activity is also of great interest. The mass spectrometer will be used to determine the composition of the atmosphere. In this context, Anderson [47] discusses the conditions of atmospheric-composition measurements in two possible models characterized by high nitrogen (5%) or argon (40 m-atm) contents, respectively. The mass-spectrometer measurements will make it possible to detect components whose concentrations exceed 10-50 ppm (to ensure purity in the atmospheric-component measurements, they will be made during the first three days, before soil-sample analysis is started). Measurements of the water content in the soil samples (with phase-state differentiation) are to be made by combined use of "scanning" calorimetry as the specimens are heated and gas analysis of the evaporating components. The presence of ice, liquid water, adsorbed films, and mineral hydrates can be detected from the correlation between the thermal anomalies and the composition of the liberated gas. Measures that ensure exclusion of fouling effects produced by the lander and its engine will be important here. /56

Composition variations of the gaseous soil component are, as a rule, an indicator of biological processes and can easily be measured by gas chromatography. The "Viking" lander is therefore to carry out an experiment whose object is to place a Martian soil sample in a culture medium and to follow this up

with an extended gas analysis of the medium over the sample for the components H_2, N_2, O_2, CH_4, K and CO_2 [48]. This type of analysis is to be carried out three times with substitution of fresh culture medium for each of the "incubation" cycles (Martian air, krypton, and water are added to the soil sample). If no changes in the composition of the medium are observed, another soil sample will be given a similar analysis. If the result is positive, it is proposed that the measurements with the first sample be continued. All measurements will be made at room temperature ($20\pm2°C$).

As one of the methods of detecting life on Mars, it has been proposed that compounds present in the soil samples be "tagged" with radiactive isotopes for analysis of metabolic activity [49]. This experiment proceeds from the following assumptions: 1) if microorganisms exist, they may assimilate the tagged substances and produce a radioactive gas; 2) biochemical reactions must be "aqueous" at the cellular level. The tagged substances will be chosen with consideration of theoretical biological data and the results of research done on the ground. Such substances should contain simple carbon compounds and (or) sulfates. The excreted gaseous products to be analyzed might be $^{14}CO_2$ and $H_2{}^{35}S$. The use of radioactive isotopes will produce results much more quickly than conventional microbiological analyses. Laboratory studies have indicated the possibility of using radioactive isotopes for analysis of cultures containing fewer than 25 cells and soil samples containing about 200 cells per milligram of sample weight. It is suggested that this experiment be continued for 15 days. In the event of a negative result, it would be repeated with a different soil sample. An experiment with a specimen held at 160°C for 3 hours for biological deactivation is planned as a control.

The principal purpose of a carbon-assimilation experiment [50] is to perform a biological analysis of Martian soil samples under the conditions of the Martian environment. This experiment is based on the assumptions that life on Mars (if it exists) is "carbon" life, and that an exchange of carbon with the atmosphere is one its manifestations (as on the earth). The Martian atmosphere contains two compounds that are highly important from the biological standpoint: carbon monoxide and carbon dioxide. The carbon content in these gases (^{14}CO and $^{14}CO_2$) will therefore be measured as an organic function of the Martian soil. On the earth, as we know, photosynthesis is the principal mechanism that fixes carbon from atmospheric carbon dioxide. On Mars, carbon monoxide formed in the atmosphere by ultraviolet photolysis of carbon dioxide may be an important

/57

source of carbon. Laboratory tests have shown that the proposed method is capable of detecting 10^2-10^3 single-cell algae or 10^5-10^6 nonphotosynthetic bacteria in a specimen. One variant of the biological analysis proposes to introduce water with the purpose of detecting products of vital activity of the terrestrial type.

The "Viking" scientific program is a good illustration of the prospects for study of Mars and demonstrates clearly the advantages of coordinated studies, which permit use of many divisions of the program for more than one purpose. From the viewpoint of pure meteorological research, data on the properties of the soil and the interaction of the atmosphere with the surface will be very important. They will, for example, make it possible to develop parameterization methods for boundary-layer processes, which are needed to construct a theory of the general atmospheric circulation. Serious attention must be given to study of cloud and haze layers, as well as dust storms and the conditions under which they form. All of this research will not only aid us in understanding the laws of the Martian weather, but also to obtain results that are of great interest for deeper understanding and forecasting of the weather on the earth.

REFERENCES

/58

1. Atmosfery Marsa i Venery (The Atmospheres of Mars and Venus). Collection of Articles (Translations from the English Edited by K.Ya.Kondrat'yev). Leningrad, Gidrometeoizdat, 1970.
2. Konashenok, V.N. and K.Ya.Kondrat'yev. Novoye o Venere i Marse (News of Venus and Mars). Leningrad, Gidrometeoizdat, 1970.
3. Marov, M.Ya. and O.L. Ryabov. Model' Atmosfery Venery (A Model of the Atmosphere of Venus). Institute of Applied Mathematics of the USSR Academy of Sciences, Moscow, Izd. IPM, Rotaprint, 1972.
4. Moroz, V.I. and L.V. Ksanfomaliti. News from Mars. "Zemlya i Vselennaya," 1972, No. 3.
5. Ohring, G. The Weather on the Planets (Russian translation), Leningrad, Gidrometeoizdat, 1968.
6. Lewes, J.S. Atmosphere, Clouds and Surface of Venus. Amer. Sci., Vol. 59, No. 5, 1971.
7. Budyko, M.I. Vliyaniye Cheloveka na Klimat (The Influence of Man on the Climate). Leningrad, Gidrometeoizdat, 1972.
8. Berlyand, M.Ye.and K.Ya. Kondrat'yev. Goroda i Klimat Planety (Cities and the Planetary Climate). Leningrad, Gidrometeoizdat, 1972.
9. Golitsyn, G.S. Estimates of Certain Characteristics of General Circulation in the Atmospheres of Planets of the Terrestrial Group. Izv. Akad. Nauk SSSR, Ser. Fizika Atmosfery i Okeana, 1968, Vol. IV, No. 11.
10. Kondrat'yev, K.Ya. Solar Constant. "Meteorologiya i Gidrologiya," 1971, No. 3.
11. Moroz, V.I. et al. Preliminary Results of "Mars 3" Spaceprobe Measurements of the Infrared Temperature of the Martian Surface. Dokl. Akad. Nauk. SSSR, 1973, Vol. 208, No. 2.
12. Science, Vol. 175, No. 40.19, 1972; Icarus, Vol. 12, No. 1, 1970.
13. Hord, C.W. "Mariner 6 and 7" Ultraviolet Spectrometer Experiment: Photometry and Topography of Mars. Icarus, Vol. 16, No. 2, 1972.
14. Kliore, A.J. et al. Atmosphere and Topography of Mars from "Mariner 9" Radio Occultation Measurements. COSPAR, Madrid, June 1972.
15. Herr, K.C. et al. Martian Topography from the "Mariner 6 and 7" Infrared Spectra. Astron. J., Vol. 75, 833-894, 1970.
16. Downs, G.S. et al. Martian Topography and Radar Brightness: The 1971 Opposition. COSPAR, Madrid, June 1972.
17. Pettengill, G.H., A.E.E. Rodgers and I.I. Shapiro. Topography and Radar Scattering Properties of Mars. COSPAR, Madrid, June 1972.

18. Hord, C.W., C.A. Barth, A.I. Stewart and A.L. Lance. "Mariner 9" Ultraviolet Spectrometer Experiment: Photometry and Topography of Mars. Icarus, Vol. 17, No. 2, 1972.
19. Barth, C.A. Ultraviolet Spectroscopy of Mars. COSPAR, Madrid, June 1972.
20. Barth, C.A., C.W. Hord and A.I. Stewart. "Mariner 9" Ultraviolet Spectrometer Experiment: Observations of Ozone on Mars. Laboratory for Atmospheric and Space Physics. Univ. of Colorado, Boulder, Colorado, 1972.
21. Lane, A.L. Ultraviolet Observations of Ozone on Mars. COSPAR, Madrid, June 1972.
22. Stewart, A.I., C.A. Barth and C.W. Hord. "Mariner 9" Ultraviolet Spectrometer Experiment: Structure of Mars' Upper Atmosphere. Laboratory for Atmospheric and Space Physics. Univ. of Colorado, Boulder, Colorado, 1972.
23. Thomas, C.E. Neutral Composition of the Upper Atmosphere of Mars as Determined from the "Mariner" UV-Spectrometer Experiment. J. Atmos. Sci., Vol. 28, No. 5, 1971, pp. 589-868.
24. Barth, C.A., A.I. Stewart, C.W. Hord and A.L. Lance. "Mariner 9" Ultraviolet Spectrometer Experiment: Mars Airglow Spectroscopy and Variations in Lyman Alpha. Icarus, Vol. 17, No. 2, 1972. /59
25. Stewart, A.I. "Mariner 6 and 7" Ultraviolet Spectrometer Experiment: Implications of CO_2^+, CO and O Airglow. J. Geophys. Res., Vol. 77, No. 1, 1972.
26. Leovy, C.B. and Y. Mintz. Numerical Simulation of the Atmospheric Circulation and Climate of Mars. J. Atmos. Sci., Vol. 26, No. 6, 1969.
27. De Vaucouleurs, G. Geometric and Photometric Parameters of the Terrestrial Planets. Icarus, Vol. 3, 1964, p. 187.
28. Kellogg, W. and C. Sagan. The Atmospheres of Mars and Venus (Russian translation), Moscow, Izd. Inostr. Lit., 1962.
29. Slipher, E.C. A Photographic History of Mars. Lowell Observatory. Flagstaff, Arizona (Library of Congress, Catalog No. 62-21127, 168 p.), 1962.
30. Gierasch, P.J. and R.M. Goody. The Effect of Dust on the Temperature of the Martian Atmosphere. J. Atmos. Sci., Vol. 29, No. 2, 1972.
31. Kondrat'yev, K.Ya, A.M. Bunakova and M.V. Anolik. Features of the Thermal Radiation Fields of the Atmospheres of Mars and Venus. In Collection Entitled "Perenos Izlucheniya v Atmosfere" (Radiation Transfer in the Atmosphere), Izd. LGU, 1972.
32. Kondrat'yev, K.Ya. and A.M. Bunakova. An Attempt at Evaluation of the Mars Thermal Radiation Field. In Collection Entitled: "Problemy Fiziki Atmosfery" (Problems of Atmospheric Physics), Izd. LGU, 1972, No. 10.

33. Kondratyev, K.Ya, A.M. Bunakova and Yu.M. Timofeev. Outgoing Thermal Radiation as an Information Source on the Composition of the Martian Atmosphere. Paper Presented to the COSPAR, Madrid, June 1972.
34. Tatom, F.B. et al. Prediction of the Martian Thermal Environment. AIAA Paper, No. 749, 1968.
35. Bartko, E. and R.A. Hanel. Non-Gray Equilibrium Temperature Distributions Above the Clouds of Venus. Astrophys. J., Vol. 151, No. 1, 1968.
36. Golubitskiy, B.M. and N.I. Moskalenko. Spectral Transmission Functions in the H_2O Vapor and CO_2 Bands. Izv. Akad. Nauk SSSR, Ser. Fizika Atmospery i Okeana, 1968, Vol. IV, No. 3.
37. Hanel, R.A. and B.J. Conrath et al. Infrared Spectroscopy Experiment on the "Mariner 9" Mission: Preliminary Results. Science, Vol. 175, No. 4019, 1972.
38. Parkinson, T.D. and D.M. Hunten. Martian Dust Storm: Its Depth on 25 November 1971. Science, Vol. 175, No. 4019, 1972.
39. Kunde, V.G. Theoretical Molecular Line Absorption of CO_2 in Late-Type Atmospheres. Astrophys. J., Vol. 153, pp. 435-450, 1968.
40. Drayson, R.S. and C. Young. The Frequencies and Intensities of Carbon Dioxide Absorption Lines Between 12 and 18 Microns. University of Michigan Technical Report 08183-1-T, 1967.
41. Gierash, P. and R.A. Goody. A Study of the Thermal and Dynamical Structure of the Martian Lower Atmosphere. Planetary and Space Sci., Vol. 16, 1968, p. 615.
42. Hanel, R.A. et al. Infrared Spectroscopy Experiment on the "Mariner 9" Mission: Preliminary Results. Science, Vol. 175, No. 4019, 1972.
43. Hess, S.L. et al. Meteorology Experiments: The Viking Mars Lander. Icarus, Vol. 16, No. 1, 1972, pp. 196-204.
44. Nier, A.O. et al. Entry Science Experiments for Viking 1975. Icarus, Vol. 16, No. 1, 1972, pp. 74-91.
45. Kiffer, H.H. et al. Infrared Thermal Mapping Experiment: the Viking Mars Orbiter. Icarus, Vol. 16, No. 1, 1972, pp. 217-222.
46. Shorthill, R.W. et al. Martian Physical Properties Experiments: the Viking Mars Lander. Icarus, Vol. 16, No. 1, 1972, pp. 217-222.
47. Anderson, D.M. et al. Mass-Spectrometric Analysis of Organic Compounds, Water and Volatile Constituents in the Atmosphere and Surface of Mars: the Viking Mars Lander. Icarus, Vol. 16, No. 1, 1972, pp. 111-138.
48. Oyama, V.I. The Gas Exchange Experiment for Life Detection: the Viking Mars Lander. Icarus, Vol. 16, No. 1, 1972, pp. 167-184.

49. Levin, G.V. Detection of Metabolically Produced Labeled Gas: the Viking Mars Lander. Icarus, Vol. 16, No. 1, 1972, pp. 153-166.
50. Horowitz, N.H., J.S. Hubbard and G.L. Hobby. The Carbon Assimilation Experiment: the Viking Mars Lander. Icarus, Vol. 16, No. 1, 1972, pp. 147-152. /60
51. Ginzburg, A.S. and Ye.M. Feygel'son. Certain Patterns of Radiative Heat Transfer in Planetary Atmospheres. Izv. Akad. Nauk SSSR, Ser. Fizika Atmosfery i Okeana, 1971, Vol. VII, No. 4.
52. Gierasch, P., R. Goody and P. Stone. Energy Balance of Planetary Atmosphere. J. Fluid Dynamics, Vol. 1, No. 1, 1970.
53. Kondrat'yev, K.Ya. and V.N. Konashenok. Theoretical Foundations of the Meteorology of Planetary Atmospheres. In Collection Entitled: "Problemy Fiziki Atmosfery" (Problems of Atmospheric Physics), Izd. LGU, 1970, No. 8.
54. Soviet Robots Investigate Mars. "Pravda", No. 238 (19746), 25 August 1972.
55. Carlson, T.N. and J.M. Prospero. The Large-Scale Movement of Saharan Air Outbreaks Over the Northern Equatorial Atlantic. J. Appl. Meteorol., Vol. 11, No. 2, 1972.
56. Golitsyn, G.S. and S.S. Zilitinkevich. Estimation of the Global Characteristics of the Circulation of the Planetary Atmosphere with Various Hypotheses as to the Nature of Dissipation. Izv. Akad. Nauk SSSR, Ser. Fizika i Okeana, 1972, Vol. VIII, No. 8.
57. Zilitinkevich, S.S. et al. Numerical Modeling of the Circulation of the Venusian Atmosphere. Dokl. Akad. Nauk SSSR, 1971, Vol. 197, No. 6.
58. Binder, A.B. and J.C. Jones. Spectrophotometric Studies of the Photometric Function, Composition, and Distribution of the Surface Materials of Mars. J. Geophys. Res., Vol. 77, No. 17, 1972.
59. Hammond, A.L. Mars as an Active Planet: the View from "Mariner 9". Science, Vol. 175, No. 4019, 1972.
60. Prokof'yeva, V.V. et al. Cloud Formations on Mars in the Summer of 1969. Astronomicheskiy Tsirkulyar, No. 635, 14 July 1971.
61. Leovy, C. Radiative Convective Equilibrium Calculations for a Two-Layer Mars Atmosphere. RM-5017-NASA. The Rand Corporation, 1966.
62. Pang, K. and C.W. Hord. Experiment with Ultraviolet Spectrometer on "Mariner 7": Photometric Function and Surface Roughness of Martian Polar cap. Icarus, Vol. 15, No. 3, 1971.
63. Stone, P.H. A Simplified Radiative-Dynamical Model for the Static Stability of Rotating Atmospheres. J. Atmos. Sci., Vol. 29, No. 3, 1972.

64. McElroy, M.B. Mars: An Evolving Atmosphere. Science, Vol. 175, No. 4020, 1972.
65. Bolle, H.J. Fine Structure Calculations of Martian CO_2 Emission Spectrum. Moon and Planets. North-Holl. Publ. Co., Amsterdam, 1970, pp. 300-313.
66. Hieronymus, W.S. Mars Seen as a "Living" Planet. Aviat. Week and Space Technol., Vol. 96, No. 9, 1972.
67. Wells, R.A. Mars: Are Observed White Clouds Composed of H_2O? Nature, Vol. 238, No. 5363, 1972, pp. 324-326.
68. Smith, S.A. and B.A. Smith. Diurnal and Seasonal Behavior of Discrete White Clouds on Mars. Icarus, Vol. 16, No. 3, 1972, pp. 509-521.
69. Horn, D. et al. The Composition of the Martian Atmosphere Minor Constituents. Icarus, Vol. 16, No. 3, 1972, pp. 543-556.
70. Owen, T. and C. Sagan. Minor Constituents in Planetary Atmospheres: Ultraviolet Spectroscopy from the Orbiting Atmospherical Observatory. Icarus, Vol. 16, No. 3, 1972, pp. 557-568.
71. Bashilova, I. and G. Makhin. Mars in the Eyes of the Geologists. Nauka i Zhizn', No. 9, 1972, pp. 45-47.
72. Leovy, C.B. et al. "Mariner 9" Television Experiment: Progress Report on Studies of the Mars Atmosphere. IAU/URSI Symposium on Planetary Atmospheres and Surfaces. Madrid, May 1972.
73. Hanel, R.A. et al. Investigation of the Martian Environment by Infrared Spectroscopy on "Mariner 9". Preprint X-620-72-280. Goddard Space Flight Center, July 1972.
74. Moroz, V.I. and L.V. Ksanfomaliti. Preliminary Results of the Astrophysical Observations of Mars from AIS Mars-3. Preprint of Paper Presented at URSI/IAU/COSPAR Symposium on Planetary Atmosphere and Surfaces, Madrid, 10-13 May 1972. /61
75. Klior, A.J. et al. The Atmosphere of Mars from "Mariner 9" Radio Occultation Experiment. Icarus, Vol. 17, No. 2, 1972.
76. Pang, K, and C.W. Hord. 1971 Mars' Duststorm. Laboratory for Atmospheric and Space Physcis. Univ. of Colorado, 1973.
77. Leovy, C. et al. The Martian Atmosphere: "Mariner 9" Television Experiment Progress Report. Icarus, Vol. 17, No. 2, 1972, p. 373.
78. Barth, C.A. et al. Seasonal Variation of Ozone on Mars. Laboratory of Atmospheric and Space Physics, Univ. of Colorado, 1973.
79. Dementyeva, N.N. Preliminary Results of Measurements of UV-Emissions Scattered in the Martian Upper Atmosphere. Icarus, Vol. 17, No. 2, 1972, p. 475.

80. Strickland, D.J. et al. "Mariner 6 and 7" Ultraviolet Spectrometer Experiment: Analysis of the OI 1304- and 1356-A Emissions. J. Geophys. Res., Vol. 77, No. 22, 1972, p. 4052.
81. Conrath, B. et al. Atmospheric and Surface Properties of Mars Obtained by Infrared Spectroscopy on "Mariner 9". Preprint NASA/GSFC X-620-72-486, December 1972.
82. Blumsack, S.L. and P.J. Gierash. Mars: the Effect of Topography on Baroclinic Instability. J. Atmos. Sci., Vol. 29, No. 6, 1972, pp. 1081-1089.

Translated for the National Aeronautics and Space Administration by Scripta Technica, Inc. NASw-2484,

NASA-Langley, 1974